NeuroImage 226 (2021) 117569

Contents lists available at ScienceDirect

NeuroImage

journal homepage: www.elsevier.com/locate/neuroimage

Learning dynamics of electrophysiological brain signals during human fear conditioning

Matthias F.J. Sperl[a,b,*], Adrian Wroblewski[c], Madeleine Mueller[c,d], Benjamin Straube[c], Erik M. Mueller[a]

[a] Department of Psychology, Personality Psychology and Assessment, University of Marburg, 35032 Marburg, Germany
[b] Department of Psychology, Clinical Psychology and Psychotherapy, University of Giessen, 35394 Giessen, Germany
[c] Department of Psychiatry and Psychotherapy, Translational Neuroimaging Marburg, University of Marburg, 35039 Marburg, Germany
[d] Department of Systems Neuroscience, University Medical Center Hamburg-Eppendorf, 20246 Hamburg, Germany

ARTICLE INFO

Keywords:
Sequential-set fear conditioning
EEG
C1
P1
N170
LPP

ABSTRACT

Electrophysiological studies in rodents allow recording neural activity during threats with high temporal and spatial precision. Although fMRI has helped translate insights about the anatomy of underlying brain circuits to humans, the temporal dynamics of neural fear processes remain opaque and require EEG. To date, studies on electrophysiological brain signals in humans have helped to elucidate underlying perceptual and attentional processes, but have widely ignored how fear memory traces *evolve* over time. The low signal-to-noise ratio of EEG demands aggregations across high numbers of trials, which will wash out transient neurobiological processes that are induced by learning and prone to habituation. Here, our goal was to unravel the plasticity and temporal emergence of EEG responses during fear conditioning. To this end, we developed a new sequential-set fear conditioning paradigm that comprises three successive acquisition and extinction phases, each with a novel CS+/CS- set. Each set consists of two different neutral faces on different background colors which serve as CS+ and CS-, respectively. Thereby, this design provides sufficient trials for EEG analyses while tripling the relative amount of trials that tap into more transient neurobiological processes. Consistent with prior studies on ERP components, data-driven topographic EEG analyses revealed that ERP amplitudes were potentiated during time periods from 33–60 ms, 108–200 ms, and 468–820 ms indicating that fear conditioning prioritizes early sensory processing in the brain, but also facilitates neural responding during later attentional and evaluative stages. Importantly, averaging across the three CS+/CS- sets allowed us to probe the temporal evolution of neural processes: Responses during each of the three time windows gradually increased from early to late fear conditioning, while long-latency (460–730 ms) electrocortical responses diminished throughout fear extinction. Our novel paradigm demonstrates how short-, mid-, and long-latency EEG responses change during fear conditioning and extinction, findings that enlighten the learning curve of neurophysiological responses to threat in humans.

1. Introduction

Rapid learning about threats is essential for survival (LeDoux and Daw, 2018), but it can also contribute to the etiology and maintenance of pathological fear (Parsons and Ressler, 2013). Patients with anxiety disorders exhibit elevated fear conditioning and resist fear extinction (Lissek et al., 2005; Duits et al., 2015). Fear conditioning (LeDoux, 2014) describes a learning procedure during which an initially neutral stimulus (conditioned stimulus, CS) elicits fear after becoming associated with an aversive event (unconditioned stimulus, US). Conversely, when the CS is presented in the absence of the aversive US, the fear response is extinguished and the strength of behavioral fear measures declines (Bouton, 2017). Neurophysiological mechanisms of fear conditioning and extinction have been widely investigated in animals (Tovote et al., 2015), leading to the development of neurobiological models of threat processing (Calhoon and Tye, 2015; McCullough et al., 2016). In animals, recording intracranial electrical activity of single units allows to unravel dynamics of threat processing with high spatial and temporal precision (Fadok et al., 2017).

Translating insights from animal studies on neural threat circuits into the human realm is challenging (Janak and Tye, 2015; Flores et al., 2018; Haaker et al., 2019): Available methods like fMRI or EEG lack either temporal or spatial specificity, respectively (Logothetis et al., 2001; Hajcak et al., 2019). Several studies have used fMRI to reveal

* Corresponding author at: Gutenbergstr. 18, 35032 Marburg, Germany.
E-mail addresses: matthias.sperl@staff.uni-marburg.de (M.F.J. Sperl), adrian.wroblewski@med.uni-marburg.de (A. Wroblewski), mad.mueller@uke.de (M. Mueller), benjamin.straube@staff.uni-marburg.de (B. Straube), erik.mueller@staff.uni-marburg.de (E.M. Mueller).

https://doi.org/10.1016/j.neuroimage.2020.117569
Received 15 June 2020; Received in revised form 13 September 2020; Accepted 10 November 2020
Available online 20 November 2020

the anatomy of fear conditioning in humans, including the amygdala (Greco and Liberzon, 2016; but see Fullana et al., 2016), insula, hippocampus, and prefrontal areas (Fullana et al., 2016). Imaging techniques like fMRI are well suited to study slower brain processes, but the study of fast and transient cortical processes requires techniques with a much higher temporal resolution. Importantly, EEG or MEG offer perfect temporal accuracy to detect changes in brain activity over milliseconds (Miskovic and Keil, 2012). These methods allow to disentangle individual neural mechanisms (Erickson et al., 2018) and to assess whether amplified cortical responses are processed at automatic or rather strategic stages (Klumpp and Shankman, 2018).

Prioritized processing of threat cues can occur at different sensory and cognitive levels (Gupta et al., 2019; Wieser and Keil, 2020), including sharpened tuning of visuocortical neurons (Stegmann et al., 2020). Electromagnetic methods are pivotal tools to investigate how threat can guide perceptual, attentional, and evaluative processing stages (Lang and Bradley, 2010; Bublatzky and Schupp, 2012; Miskovic and Keil, 2012). Some studies suggest that fear conditioning facilitates neural processing at very early stages which begin already at latencies < 40 ms after stimulus onset (Bröckelmann et al., 2011; Kluge et al., 2011; Morel et al., 2012; Steinberg et al., 2013). Others reported heightened parieto-occipital amplitudes to CS+ versus CS- from 60 to 90 ms (Stolarova et al., 2006; Hintze et al., 2014; Thigpen et al., 2017) as indicated by the C1 component amplitude. These results emphasize that short-term plasticity in primary visual neurons may be responsible for biased threat perception already during early latencies. A few studies propose that conditioned responses amplify amplitudes of the P1 (~80–150 ms) and of the face-sensitive N170 (~130–200 ms) components (Pizzagalli et al., 2003; Pourtois et al., 2004; Liu et al., 2012b; Levita et al., 2015; Camfield et al., 2016; Muench et al., 2016), but results are mixed. Specifically, Muench et al. (2016) showed more positive P1 amplitudes at lateral parietal electrode sites for fear-conditioned faces, but only during a self-relevant threat context. Levita et al. (2015) and Camfield et al. (2016) found more negative amplitudes at occipito-temporal channels and interpreted these effects as elevated N170 responses. However, other studies failed to replicate differential fear responses during these mid-latency periods (Stolarova et al., 2006; Seligowski et al., 2018; Stolz et al., 2019), and inconsistent findings (Schindler and Bublatzky, 2020) may arise from increased attention toward both threat (CS+) and safety (CS-) cues (Bublatzky and Schupp, 2012).

Wieser and Keil (2020) argue that modulations of the C1, P1, and N170 amplitudes reflect neural correlates of a somewhat “broad” discrimination between threat and non-threat cues. In contrast, effects on late-latency (> 300 ms) event-related potential (ERP) components are assumed to indicate sustained activation of motivational neural systems (Cuthbert et al., 2000; Hajcak and Foti, 2020), related to widespread perceptual, motivational, and motor signals (Wieser and Keil, 2020). Numerous studies confirmed that the late positive potential (LPP) at parieto-occipital sensors is reliably enhanced to fear-conditioned stimuli (Panitz et al., 2015, 2018; Pastor et al., 2015; Bacigalupo and Luck, 2018; Seligowski et al., 2018; Ferreira de Sá et al., 2019; Pavlov and Kotchoubey, 2019; Stolz et al., 2019). The exact time window for LPP scoring varies between studies, but the majority restricted statistical analyses to the 300–800 ms period.

Taken together, EEG studies have not only reported that fear conditioning modulates rather early (Miskovic and Keil, 2012) ERP components (which can be interpreted as facilitated perception through early visual cortical plasticity), but also found effects on later (Panitz et al., 2015; Bacigalupo and Luck, 2018) ERP components (reflecting sustained engagement with threat). All of these results typically rely on averaging across a massive number of trials to achieve an acceptable signal-to-noise ratio for EEG (Huffmeijer et al., 2014), thereby neglecting any changes in the course of learning that would be expected from theoretical models (Rescorla and Wagner, 1972). Notably, neurophysiological responses to the CS change across trials due to habituation and learning. For example, single-trial analyses suggest that P1 modulations change throughout fear conditioning, depending on involved attention mechanisms (Liu et al., 2012b). These temporal dynamics are often of particular interest and considered in fMRI studies (Yin et al., 2018). When averaging across all EEG trials of an acquisition session, however, any information about the learning dynamics within that session will typically be lost. Furthermore, modulation of transient ERP components can be overlooked due to habituation across many trials.

During the last decade, a growing body of studies has begun to translate electrophysiological signatures of learned fear from the rodent model to humans (e.g., Thigpen et al., 2017; Bacigalupo and Luck, 2018; Seligowski et al., 2018; Roesmann et al., 2020). Although learning may be defined as a *change in neural activity* due to experience (Ferreira de Sá et al., 2019), human electrophysiological studies of fear conditioning have widely been unable to investigate how brain signals to threat stimuli actually *change* over the course of learning. To close this gap and to overcome the methodological challenges described above, we developed a new sequential-set fear conditioning paradigm that comprises three successive acquisition phases, each with a *novel* CS+/CS- set. We validated our new paradigm by means of a data-driven approach to identify differences in EEG topography between experimental conditions and by testing whether fear conditioning effects in one stimulus set are also present across the other two with regard to EEG components, subjective ratings, electrodermal activity, and fear bradycardia. As outlined above, findings on the timing of ERP effects during fear conditioning are heterogeneous, and, for some components (e.g., P1 and N170), results diverge (Pizzagalli et al., 2003; Ferreira de Sá et al., 2019). The majority of studies focused on specific *a priori* selected components, with latencies and electrodes varying across studies. Thereby, this approach makes the selection of parameters a somewhat speculative endeavor, which may result in missing any effects that do not align with *a priori* selected latencies and electrodes. To address this issue, we applied a data-driven approach to identify relevant time windows for ERP analyses. Following previous fear conditioning studies, we were specifically interested in ERP responses within 1000 ms.

Our new sequential-set fear conditioning paradigm allows probing the temporal unfolding of brain mechanisms with EEG, thereby complementing functional anatomical knowledge obtained from fMRI research. On the one hand, averaging across trials from three CS sets ensures a high signal-to-noise ratio. On the other hand, by using three CS sets there are fewer repetitions of a single stimulus. Importantly, our paradigm triples the relative amount of trials that capture habituation-prone neural responses given that *novel* pictures have been shown to lead to a complete recovery of attenuated ERP amplitudes (Codispoti et al., 2006, 2007). While reducing habituation, sequential-set conditioning should therefore ensure a good signal-to-noise ratio for tapping into more transient neurophysiological processes. Specifically, we hypothesized that from early to late fear conditioning trials ERP amplitudes would gradually increase to CS+ versus CS-, particularly within the aforementioned time windows and locations roughly relating to the C1, P1, N170, and LPP components. Conversely, CS+ versus CS- differences in ERP amplitudes should vanish throughout fear extinction.

2. Materials and methods

2.1. Participants

Twenty-four healthy, right-handed, and non-smoking students at the University of Marburg participated in this study. One subject did not complete the study, and two subjects were excluded because of excessive artifacts in EEG data, yielding a total sample of $N = 21$ participants (mean age = 20.76 years, $SD = 2.28$ years, range: 18–26 years; 85% females). Based on our previous studies (e.g., Panitz et al., 2018; Stolz et al., 2019), we expected medium to large effect sizes for conditioned fear responses. Thus, we used G*Power (Faul et al., 2007) to determine the sample size needed for an effect size of Cohen’s $d = 0.7$.

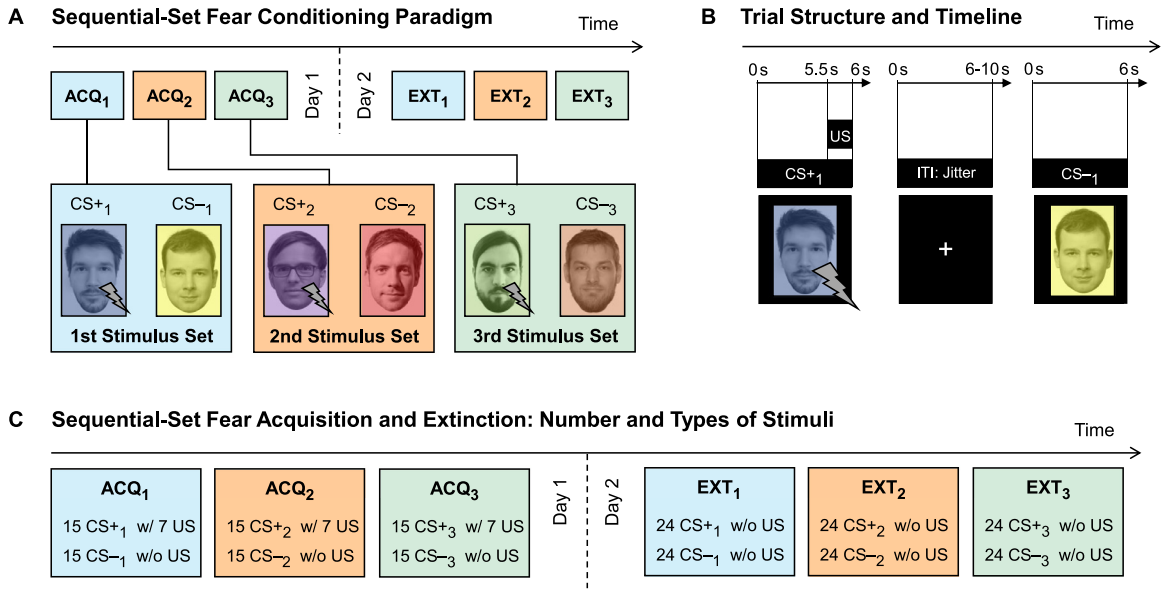

Fig. 1. Sequential-set fear conditioning paradigm. (A) Participants underwent three successive acquisition training phases (ACQ_1, ACQ_2, and ACQ_3), each with a novel conditioned stimulus (CS+/CS-) set (differently tinted neutral faces). For instance, the $CS+_1/CS-_1$ stimulus set was used during the first acquisition training (ACQ_1). Approximately 24 h after fear conditioning, subjects underwent sequential-set extinction, which consisted of three successive extinction training phases (EXT_1, EXT_2, and EXT_3), each with the corresponding CS+/CS- set. (B) Trial structure and timeline for a single CS trial. All CSs were presented for 6 s, followed by a jittered 6–10 s intertrial interval. During acquisition training, CS+ were paired with an aversive electric shock unconditioned stimulus (US). The delivery of the US started 500 ms before the CS offset. (C) The number and stimuli types presented during the experimental phases. During three acquisition training phases, $CS+_1$, $CS+_2$, and $CS+_3$ were reinforced with an aversive US ("w/", reinforcement rate of 47%), while $CS-_1$, $CS-_2$, and $CS-_3$ were never paired with a US ("w/o"). Note: Due to licensing restrictions, we cannot publish the original stimulus material that we used in the present study. To illustrate the paradigm, panels A and B contain comparable stimuli with faces of the authors of this article and their colleagues. The original stimulus material is available upon request.

Under the assumption of a significance level of $\alpha = .05$ and a power level of $1 - \beta = .08$, *a priori* power analyses revealed that a total sample size of 19 would be required. To allow for a potential data loss of up to 20%, we recruited 24 participants.

All subjects gave written informed consent to participate. They participated for either partial fulfillment of course credit or were reimbursed with €10 per hour. Exclusion criteria were a history of cardiovascular, neurological, or mental disorders (assessed by the short version of the Diagnostic Interview for Mental Disorders, Mini-DIPS; Margraf, 1994), and regular use of either illegal drugs or prescription drugs that affect the central nervous system. All participants were asked to refrain from alcoholic or caffeinated drinks, heavy meals, and strenuous exercise prior to the experiment. The study protocol was approved by the local ethics committee of the Department of Medicine at the University of Marburg.

2.2. Experimental fear conditioning and extinction paradigm

We developed a new experimental paradigm that is designed to study the time course of electrocortical fear responses throughout fear conditioning and extinction. Our paradigm was administered over two consecutive days (see Fig. 1): Participants underwent sequential-set fear conditioning on day 1, while sequential-set fear extinction took place 24 h later on day 2. Specifically, one CS (the CS+) was paired with the aversive US, while a second CS (the CS-) remained unpaired. The differential fear response can be quantified as heightened responses to CS+ compared with CS-.

Importantly, day 1 sequential-set fear conditioning consisted of three successive acquisition training phases, each with a novel CS+/CS- set. Here, we denote each of the three sets with a subscript (i.e., $CS+_1/CS-_1$, $CS+_2/CS-_2$, and $CS+_3/CS-_3$). Specifically, each set comprised two different neutral faces on different background colors, which served as CS+ and CS-, respectively. During the acquisition training of set 1 (ACQ_1), the $CS+_1/CS-_1$ stimulus set was used, during the acquisition training of set 2 (ACQ_2), a second $CS+_2/CS-_2$ stimulus set was shown, and during the last acquisition training (ACQ_3), a third $CS+_3/CS-_3$ stimulus set was presented. During each of the three acquisition training phases, CS+ and CS- stimuli were shown 15 times each in a random order, with the CS+ paired with an aversive electric shock US during 7 trials (see Fig. 1C). To familiarize participants with the stimuli, the corresponding CS+ and CS- stimuli were presented four times during three pre-acquisition phases (pre-ACQ), which took place immediately before the respective acquisition training phase. Prior to acquisition, participants were verbally instructed to expect a shock paired with the presentation of the CS+ face (Hollandt et al., 2020). Participants were instructed about the contingency but were not informed about the reinforcement rate (Mertens et al., 2018). Note that the first CS+ during each acquisition phase was always paired with the US.

Approximately 24 h after fear conditioning, subjects underwent sequential-set fear extinction. Similar to the acquisition training procedure, day 2 fear extinction consisted of three successive extinction training phases, each with the corresponding CS+/CS- set. Specifically, during each extinction training (EXT_1, EXT_2, and EXT_3), CS+ and CS- stimuli were presented 24 times each in a random order without any US presentation (see Fig. 1C). To reactivate the CS-US contingency, a single CS+ reinforced with the electric shock US (same intensity as during day 1) and a single CS- were presented prior to each extinction training phase (Monfils and Holmes, 2018; Hollandt et al., 2020). On day 2, participants were instructed that electric shock stimuli "may occur" during the experiment.

Consistent with several studies from human (e.g., Feng et al., 2015; Ebrahimi et al., 2020; Hollandt et al., 2020) and animal (e.g., Voulo and Parsons, 2017; Ramanathan et al., 2018; Hartley et al., 2019) literature, fear conditioning and extinction were separated by approximately 24 h to allow fear memory consolidation prior to extinction training. There is robust evidence that sleep plays a pivotal role in the consolidation of fear-conditioned memories (Kumar et al., 2012; Pace-Schott et al., 2015; Menz et al., 2016). If fear conditioning and extinction are performed on

the same day, extinction learning is likely to interfere with fear memory consolidation, resulting in the so-called "immediate extinction deficit" (Maren, 2014).

2.3. Conditioned and unconditioned stimuli

Following previous studies, pictures of male faces with a neutral expression and tinted in either blue, yellow, purple, red, green, or orange color (as used by Klumpers et al., 2010; Duits et al., 2017; Heinig et al., 2017; Hollandt et al., 2020; see Fig. 1A and B) served as CSs. Photos of six male faces were selected from the Psychological Image Collection at Stirling (http://pics.psych.stir.ac.uk; nottingham_scans set; ids: m025, m051, m064, m095) and from the NimStim stimulus set (Tottenham et al., 2009; ids: 27M_NE_C, 36M_NE_C). All CS faces (size: 13.5 × 18 cm) were presented on a 24-in computer monitor placed approximately 50 cm in front of the participant. The stimuli were shown for 6 s, using the computer program Presentation 18.2 (Neurobehavioral Systems, Berkeley, CA/USA). During a jittered intertrial interval (defined as CS offset to CS onset) of 6–10 s, a white fixation cross was shown on a black background (see Fig. 1B). The assignment of face stimuli to CS+ and CS- was counterbalanced.

The US consisted of a 500-ms multipulse (100 single 5-ms pulses) percutaneous electrical stimulation. US presentation started 5.5 s after CS onset. Electrical stimulation was delivered from a constant current stimulator (DS7A; Digitimer Ltd., Welwyn Garden City, UK; 400 V maximal voltage) using two steel disk electrodes (Technomed Europe, Maastricht, The Netherlands; 8-mm diameter, 23 mm apart) attached to the inside of the left forearm, about 11 cm from the carpus. During a work-up procedure (a detailed protocol is available at https://doi.org/10.5281/zenodo.4294603), we presented electrical stimuli at increasing intensities until the shocks were subjectively perceived as "difficult to bear, but acceptable" ($M = 1.84$ mA, $SD = 0.76$ mA). Using these relatively high shock intensities, we have already shown successful fear conditioning on physiological and subjective levels in a previous simultaneous EEG-fMRI study (Sperl et al., 2019). Shock electrodes were attached during all experimental stages.

2.4. Subjective CS ratings

Prior to and after each experimental stage, participants were asked to indicate the US expectancy ("How likely is it that the electric stimulus will coterminate with this picture?") for each CS on an 11-point numeric rating scale ranging from 0% ("US will definitely not coterminate") to 100% ("US will definitely coterminate"). Furthermore, participants rated the subjective valence ("How good or bad do you feel when looking at this picture?"; 0 = "very good" to 100 = "very bad") and arousal ("How aroused do you feel when looking at this picture?"; 0 = "not aroused at all" to 100 = "extremely aroused") of their current feeling on an 11-point scale. In order to assess the temporal dynamics of extinction learning over trials (Golkar et al., 2013), each extinction training phase was split into three blocks. Additional subjective CS ratings were obtained between these blocks.

2.5. EDA data acquisition and analyses

Electrodermal activity (EDA), electrocardiogram (ECG), and electroencephalogram (EEG) were recorded at a 1024 Hz sampling rate using the BioSemi Active Two EEG system (BioSemi, Amsterdam, The Netherlands). Physiological data were low-pass filtered online with a cutoff frequency of 208 Hz. For EDA (exosomatic measurement, 1 μA at 16 Hz AC), two Ag/AgCl electrodes (5-mm diameter) filled with isotonic (0.5% NaCl) electrolyte medium were placed on the thenar and hypothenar eminences of the nondominant (left) hand. Raw EDA data were low-pass filtered (1 Hz, signal amplitude is attenuated by 3 dB at cutoff frequency, 4th order Butterworth filter, 24 dB/octave roll-off) offline in BrainVision Analyzer 2.1.2 (Brain Products, Munich, Germany) and downsampled to 128 Hz. Artifact correction and trough-to-peak analyses were performed in Ledalab 3.4.9 (Benedek and Kaernbach, 2010a, 2010b), implemented in MATLAB 9.2 (MathWorks, Natick, MA/USA). After visual data inspection, technical artifacts were corrected with spline or cubic interpolation. For each CS trial, a skin conductance response (SCR) score was calculated as the amplitude-sum of significant SCRs within 1 and 5 s after the CS onset. Given that latencies shorter than 1 s should be treated with caution (Boucsein et al., 2012), SCRs during the first second after CS onset were omitted. SCRs smaller than 0.01 μS were considered zero responses. To obtain a normal distribution, SCR scores were logarithmized, $\ln(\mu S+1)$, before averaging. SCR scores were then averaged across trials for each CS type. Both unreinforced and reinforced CS+ trials were included because the SCR response window did not overlap with the US onset. In fact, the trial timing of our paradigm was optimized to also allow for appropriate SCR and heart period (see below) analyses. The CSs were shown for 6 s, and the US coterminated with the last 500 ms of the CS+. Compared with the majority of fear conditioning studies, the CS duration is relatively long. However, this timing ensures that the SCR response window does not overlap with the US onset. SCR amplitudes typically habituate over time, and habituation is usually weaker for CS+ versus CS- (Lonsdorf et al., 2017). If only unreinforced SCR trials are included in statistical analyses, different habituation curves for CS+ compared with CS- can be problematic and reduce statistical power. In the present study, we circumvented this shortcoming, and *all* trials could be used for statistical analyses. In addition to CS-evoked SCRs, we also analyzed responses to the US.

2.6. ECG data acquisition and analyses

For ECG, two Ag/AgCl electrodes (4-mm diameter) were filled with liquid gel and placed in Lead II configuration (right arm and left leg). Preprocessing of ECG data was performed in BrainVision Analyzer 2.1.2 (Brain Products, Munich, Germany). Raw ECG data were band-pass filtered (1–30 Hz, signal amplitude is attenuated by 3 dB at cutoff frequencies, 4th order Butterworth filter, 24 dB/octave roll-off) and notch filtered (50 ± 2.5 Hz, 16th order Butterworth filter, 96 dB/octave roll-off) offline. Afterward, R-spikes were detected automatically with the ECG Markers Solution in BrainVision Analyzer 2.1.2 (Brain Products, Munich, Germany), ECG data were manually checked for artifacts, and R-spikes were corrected if necessary. Then, we calculated a continuous heart period trace using custom-made MATLAB scripts (MATLAB 9.2; MathWorks, Natick, MA/USA). In particular, the ECG was converted to a time course of interbeat intervals (IBIs), and each IBI time point represents the latency between the pre- and succeeding R-spike in ms (Mueller et al., 2013). Next, this IBI time series was segmented into epochs ranging from −1 to 10 s relative to the onset of the CS, baseline-corrected relative to 1 s pre-CS, and averaged across trials for each CS type. In fear conditioning experiments, heart rate responses to a CS typically display a three-phasic response pattern (Lipp, 2006), starting with an initial heart rate deceleration (D1), followed by a transient acceleration (A) and a second deceleration (D2). Fear conditioning evokes a larger second deceleration component for CS+ compared with CS- (Notterman et al., 1952; Deane and Zeaman, 1958; Panitz et al., 2015). To analyze CS-evoked fear bradycardia, the maximum IBI value for the D2 period, which typically coterminates with the onset of the US (Deane and Zeaman, 1958), was extracted from 4 to 8 s after CS onset. If the distance between CS and US onsets is too short, fear-conditioned deceleration effects can be attenuated by the preceding acceleration component. As described above, we used a rather long CS-US interval, which allows to reliably disentangle decelerative (D2) from accelerative (A) cardiac responses. Fear bradycardia usually overlaps with the US onset (Deane and Zeaman, 1958). To avoid contamination by an evoked response to the US, we included only unreinforced CS+ trials for the

acquisition training phases. This approach allowed us to extend the response window beyond the US onset. We also analyzed unconditioned responses, which typically appear as cardiac acceleration (A) to an electrotactile US (Ginsberg and Thysell, 1966; Lipp, 2006; Vila et al., 2007). To quantify acceleratory responses, the minimum IBI value within 4 s after US onset was extracted.

2.7. EEG data acquisition and analyses

EEG was recorded using a 64-channel BioSemi Active Two EEG system (BioSemi, Amsterdam, The Netherlands), referenced to the common mode sense (CMS) electrode in a dynamic feedback loop with the driven right leg (DRL) electrode. The electrodes contained a sintered Ag/AgCl electrode tip. A schematic illustration of the electrode montage and scalp coordinates are available at https://doi.org/10.5281/zenodo.4294603. EEG data were preprocessed in BrainVision Analyzer 2.1.2 (Brain Products, Munich, Germany). Raw EEG data were high-pass filtered (0.5 Hz, signal amplitude is attenuated by 3 dB at cutoff frequency, 4th order Butterworth filter, 24 dB/octave roll-off) and notch filtered (50 ± 2.5 Hz, 16th order Butterworth filter, 96 dB/octave roll-off) offline. The high-pass filter was applied to remove slow drifts, which can be caused by skin potentials (Cohen, 2014), and is required for independent component analysis (ICA) to obtain reliable and valid decomposition results (Winkler et al., 2015; Dimigen, 2020). We confirmed that all results could be reproduced with different high-pass filter settings (0.5 Hz, 0.1 Hz, 0.01 Hz, no high-pass filter; see Supplementary Material A). ICA (extended infomax ICA with classic principal component analysis sphering on the whole artifact-free EEG dataset) was used for eye-blink/movement correction, and corrupted channels were interpolated using a spherical spline interpolation (Perrin et al., 1989). Afterward, data were re-referenced to the average reference. In accordance with prior research (Auerbach et al., 2016; Whitton et al., 2016; Seligowski et al., 2018; Schroder et al., 2019), we used a semi-automated procedure to reject artifact intervals, using the following criteria: (a) a voltage step exceeding 50 μV between two contiguous sampling points, (b) an absolute voltage difference of more than 150 μV within a period of 200 ms, (c) an absolute amplitude lower than −75 μV or higher than 75 μV, and (d) a maximum voltage difference of less than 0.5 μV between the maximum and minimum within a period of 100 ms. In addition to these semi-automated artifact rejection procedures, the EEG signal was visually inspected for manual artifact identification and removal by an experienced rater. All intervals that contained artifacts in at least one channel were discarded from further EEG analyses. Information on the residual number of trials per CS type after artifact rejection is provided in Supplementary Material B (see Supplementary Fig. S2). Finally, EEG was low-pass filtered (30 Hz, signal amplitude is attenuated by 3 dB at cutoff frequency, 4th order Butterworth filter, 24 dB/octave roll-off), and we computed ERPs covering 1000 ms time-locked to the CS+ and CS- onsets. ERPs were baseline-corrected (200 ms pre-stimulus) and averaged across trials. We included unreinforced and reinforced CS+ trials, as EEG epochs ended before the US onset. In addition to responses to the CSs, we also assessed US-evoked ERPs.

Traditionally, ERP analyses have mostly applied standard univariate statistics and compared waveforms at certain channels during certain time windows, often based on previous literature. However, this approach neglects the intrinsic correlation structure of EEG data (Koenig and Melie-García, 2009; Michel and Murray, 2012), which is related to redundancy in space (correlation of neighboring electrodes) and time (correlation of neighboring sampling points). This can be problematic, as traditional methods thereby often miss out on a large amount of the information which can be obtained from the EEG signal. To tackle this problem, we applied the so-called topographic analysis of variance (TANOVA) method (Murray et al., 2008; Koenig and Melie-García, 2009) in the present study. While retaining statistical rigor, this multivariate approach considers spatial and temporal information from each sensor and sampling point, respectively (Michel and Murray, 2012).

Furthermore, the exact time windows for statistical analyses on ERP differences between experimental conditions has often been selected "based on prior research" (Keil et al., 2014). However, in the fear conditioning literature, investigated ERP components (e.g., C1, P1, LPP) and exact latency windows vary strongly among studies (Pizzagalli et al., 2003; Miskovic and Keil, 2012; Ferreira de Sá et al., 2019). In addition, Luck and Gaspelin (2017) argued that the latency of observed effects may differ between studies due to low-level sensory factors (e.g., stimulus luminance and discriminability) which are often not standardized between fear conditioning studies. These discrepancies turn the selection of ERP components and adequate measurement windows into a somewhat speculative endeavor which can lead to biased conclusions (Michel and Murray, 2012; Keil et al., 2014; Clayson et al., 2019). Given these circumstances, the appropriate selection of relevant time windows is particularly challenging when validating a new paradigm. Moreover, if time windows for ERP analyses are selected *a priori*, effects (e.g., during periods of low-amplitude) can easily be overlooked (Murray et al., 2008).

Therefore, we applied a *data-driven* approach that aims to assess differences in amplitude strength and topography between experimental conditions. In contrast to "traditional" ERP analyses, this method provides a more complete insight and does not suffer from an *a priori* bias with regard to time windows and electrode locations (Murray et al., 2008; Michel and Murray, 2012). To identify relevant ERP components that are modulated by the processing of CS+ compared with CS-, we analyzed scalp ERP data with spatio-temporal electric field analyses (Lehmann and Skrandies, 1984; Murray et al., 2008). Importantly, because we were specifically interested in different electrocortical processing between CS+ and CS-, our goal was to identify continuous periods during which ERPs and topographic maps significantly differ between both CS types (Gianotti et al., 2008; Murray et al., 2008; Koenig and Melie-García, 2009). The data-driven TANOVA method tests for map differences between conditions and provides a *p*-value for each time point of the ERP trace, quantifying the strength of the difference map between CS+ and CS- conditions (Murray et al., 2008; Koenig and Melie-García, 2009). Consequently, time windows of contiguous time points with significant TANOVA results ($p \leq .05$) indicate ERP components that are modulated by CS+ compared with CS-. This method has previously been used to identify relevant ERP components that reflect differential electrocortical processing between experimental conditions (e.g., Lavric et al., 2004; Maurer et al., 2005; Martinovic et al., 2014; Bailey et al., 2019).

We performed a TANOVA as implemented in the Randomization Graphical User Interface (RAGU) software package (version 2018-10-16; Koenig and Melie-García, 2009; Koenig et al., 2011; Habermann et al., 2018), which is based on MATLAB 9.2 (MathWorks, Natick, MA/USA), to compare scalp field differences between CS+ and CS- across all EEG channels and time points. Specifically, RAGU performs randomization statistics without making any *a priori* assumptions concerning electrode sites or time windows. To obtain an accurate estimate of significance at the 5% level, 5000 randomization runs were performed (Manly, 2007; Koenig et al., 2011; Habermann et al., 2018). We used global duration statistics to control for multiple comparisons among time points. Therefore, the probability for a given effect duration under the null hypothesis is calculated. This analysis indicates a *minimum effect duration* containing time points with $p \leq .05$ that needs to be exceeded to reach "overall" significant TANOVA effects. Note that this approach efficiently controls for multiple comparisons among time points but results in highly conservative significance testing (Habermann et al., 2018). In particular, periods of early ERP effects are often short-lasting and therefore less likely to meet the critical duration for reaching significance at this "overall" level. Global duration statistics revealed a duration of 56.64 ms for acquisition and 63.48 ms for extinction, respectively. For day 1 fear conditioning, ERPs were averaged across all acquisition training trials and

all three stimulus sets to compute the TANOVA. For day 2 fear extinction, we expected a large conditioned response during the first trials and a decline toward later trials. Hence, ERPs from only the first extinction training block (i.e., the first 8 trials) from all three stimulus sets were averaged for the extinction TANOVA. In addition, we computed follow-up ANOVAs to explicitly test for the stability of the observed ERP effects across CS sets. The mean voltage following CS+ and CS- presentations within the time windows that were indicated by TANOVA was extracted separately for each stimulus set and subjected to *Contingency* x *Set* x *Channel* (x *Hemisphere*) ANOVAs. For follow-up statistical analyses, channels with the largest negative or positive deflection in the grand-grand average ERP (across CS+ and CS- trials and stimulus sets) were used.

Map differences between conditions can be produced (1) by a change in strength of similar generators ("quantitative difference of activation"), (2) by differences in source orientation or distribution ("qualitative difference"), or (3) by a combination of both (Koenig and Melie-García, 2009; Koenig et al., 2011; Habermann et al., 2018). In the present study, we were interested in both quantitative and qualitative differences between maps. Thus, our TANOVA approach tested for both effects, which offers the possibility to detect *all* (i.e., strength- *and* topography-related) systematic electrocortical differences between CS+ and CS- (Maurer et al., 2005). If, however, EEG data are normalized prior to spatio-temporal TANOVA analyses, significant map effects indicate that partially different sources ("qualitative difference") gave rise to scalp differences between conditions (Michel and Murray, 2012). To explicitly test for the influence of different generators in the brain, we also computed a second TANOVA on the amplitude-normalized maps (Koenig and Melie-García, 2009; Koenig et al., 2011; Habermann et al., 2018). To achieve data normalization, all potential values of a specific map were divided by its Global Field Power (GFP), i.e., all maps were scaled to have GFP = 1. The GFP, which is calculated as the mean absolute potential difference in the field, represents the spatial standard deviation across all electrodes at a specific time point and is considered to be a reference-free measure of response strength (Lehmann and Skrandies, 1980). Detailed analyses on amplitude-normalized maps are shown in Supplementary Material C.

2.8. Statistical analyses

For all dependent variables, we computed repeated-measures ANOVAs with the factors "*Contingency*" (CS+ versus CS-) and "*Set*" (CS set 1, 2, 3; e.g., $CS+_1/CS-_1$). Day 1 conditioning and day 2 extinction were analyzed separately.

For fear conditioning, subjective ratings (valence, arousal, and US expectancy) collected after each acquisition training phase (ACQ_1, ACQ_2, and ACQ_3) were used for ANOVAs. Similarly, we used the condition-specific average for the skin conductance response, fear bradycardia, and EEG amplitude at previously identified spatio-temporal positions (see above). The validity of the sequential-set fear conditioning paradigm would be supported by greater fear responses (i.e., higher subjective ratings, larger physiological responses) for CS+ compared with CS-, which should be comparable across all three CS sets. Thus, an increase in conditioned responses throughout fear acquisition training phases can be interpreted as successful fear conditioning.

For fear extinction, we expected a decline in conditioned responses. Hence, the factor "*Time*" referred to the affective CS ratings *before* and *after* each extinction training block, or to the mean physiological CS-evoked response *during* the respective extinction training block. For ratings and EEG data, these blocks consisted of eight trials. Due to a better signal-to-noise ratio for EDA and ECG versus EEG data (e.g., Panitz et al., 2015; Sperl et al., 2016), only four trials were averaged for peripheral physiological data to allow for more fine-grain analyses of extinction learning over time. The validity of sequential-set fear extinction would be supported by a decline in conditioned fear responses from early to late blocks for CS sets 1, 2, and 3.

Our overarching goal was to develop a paradigm that allows studying learning dynamics of neural responses within experimental stages. To account for more subtle changes in ERP responses across trials, experimental stages were split into smaller sub-blocks of five (acquisition training) or four (pre-acquisition and extinction training) trials each. Collapsing across CS sets allowed us to probe temporal changes in neural responding across trials. Importantly, this approach leads to (a) an adequate signal-to-noise ratio (through averaging *across* CS sets) while (b) creating the possibility to detect temporal changes during learning (because only a few trials need to be averaged *within* each CS set). Mean ERP responses (averaged across CS sets and across EEG channels with significant effects) were subjected to ANOVAs, including the factors "*Contingency*" (to compare CS+ with CS-) and "*Sub-Block*" (to assess temporal changes during learning). We expected an increase in conditioned electrocortical responses from early to late conditioning. Conversely, differential responses should decline throughout fear extinction. Polynomial contrasts were calculated for the *Contingency* x *Sub-Block* interactions to evaluate whether the increase (during fear conditioning) and decrease (during fear extinction) can be best described by a linear, quadratic, or cubic trend.

Significant ANOVA interactions involving the factor *Contingency* (CS+ versus CS-) were further analyzed using follow-up ANOVAs and *t*-tests. Statistical tests on physiological data (EDA, ECG, and EEG) and subjective data (subjective CS ratings of arousal, valence, and US expectancy) were performed using SPSS 24 for Windows (IBM, Armonk, NY/USA). To reach statistical significance, $p \leq .05$ was required. The Greenhouse-Geisser (1959) correction was applied for repeated-measures ANOVAs when the sphericity assumption was not met. Cohen's (1988, 1992) *d* is used to report the effect size of conditioned fear responses.

2.9. Data and code availability

De-identified data for analyses described in this manuscript along with a code-book and the data analysis scripts are publicly posted at https://doi.org/10.5281/zenodo.4294603, and are available online for interested readers.

3. Results

3.1. Subjective ratings and peripheral physiological data during fear acquisition

As expected, ANOVAs on subjective ratings of the CS after acquisition training confirmed successful fear conditioning (*Contingency* main effect, see Fig. 2A) with regard to valence, arousal, and US expectancy both across ($F(1,20) \geq 123.82$, all $ps \leq .001$, $ds \geq 2.43$) and within different CS+/CS- sets ($F(1,20) \geq 8.45$, all $ps \leq .001$). Supporting successful fear learning at the electrodermal level (see Fig. 2B), participants showed significant SCR increases to the CS+ compared with the CS- (*Contingency* main effect, $F(1,20) = 30.53$, $p < .001$, $d = 1.21$). Moreover, individual paired-samples *t*-tests (CS+ versus CS-) for CS set 1 ($t(20) = 6.48$, $p < .001$), set 2 ($t(20) = 5.37$, $p < .001$), and set 3 ($t(20) = 4.39$, $p < .001$) demonstrated higher SCRs during all three successive acquisition training phases. In line with affective CS ratings and elevated SCRs, a significant *Contingency* main effect ($F(1,20) = 21.72$, $p < .001$, $d = 1.17$) for heart period data indicated a successful acquisition of fear-conditioned bradycardia. Specifically, Fig. 2C shows that CS+ evoked a stronger cardiac deceleration compared with CS-. Moreover, *t*-tests within CS sets confirmed fear-conditioned bradycardia for CS set 1 ($t(20) = 3.76$, $p = .001$), set 2 ($t(20) = 4.16$, $p < .001$), and set 3 ($t(20) = 3.78$, $p = .001$).

In addition to conditioned fear responses, we were also interested in unconditioned physiological responses (see Fig. 2B and C). The US evoked significant SCRs (one-sample *t*-test, $\mu \neq 0$) during the acquisition training of CS set 1 ($t(20) = 6.60$, $p < .001$), set 2 ($t(20) = 5.99$, $p < .001$), and set 3 ($t(20) = 5.76$, $p < .001$). Furthermore, we observed

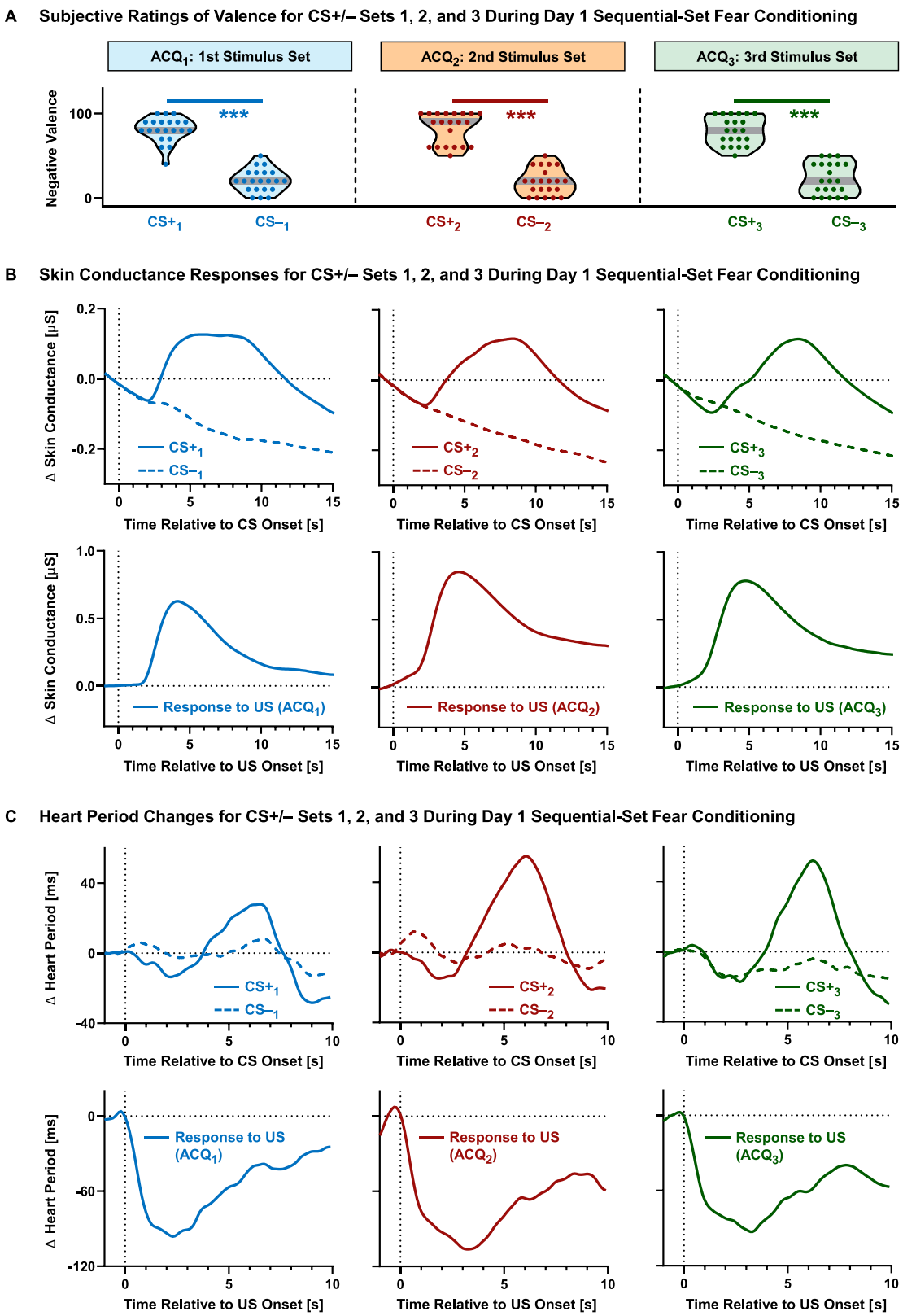

Fig. 2. Subjective and peripheral physiological (electrodermal activity and electrocardiogram) correlates of day 1 sequential-set fear conditioning. Conditioned and unconditioned responses are plotted separately for the three conditioned stimulus (CS) sets (e.g., $CS+_1$ versus $CS-_1$). (A) Ratings of CS-associated valence indicated that CS+ compared with CS- was associated with more negative valence for all three CS sets. Participants were asked to indicate their current feeling (0 = "very good" to 100 = "very bad") when looking at the faces. The results for ratings of arousal and US expectancy were similar. Violin plots display the frequency distribution of subjective ratings. Individual data points are superimposed on the violin plot, and the median is displayed as a grey horizontal line. (B) Furthermore, the CS+ (versus CS-, upper panels) and the US (lower panels) evoked increased skin conductance response (SCR) amplitudes. (C) While the CS+ (versus CS-, upper panels) is associated with relative fear bradycardia (i.e., heart period slowing), cardiac responses to the US (lower panels) showed a large acceleration component. Peripheral physiological responses were similar for all three stimulus sets. To illustrate the time series of CS- and US-evoked changes in peripheral physiological data, SCR and heart period data (interbeat intervals) were baseline-corrected (1 s pre-CS) and averaged across trials and participants. Only unreinforced CS+ trials were averaged, which allowed us to display physiological responses beyond the US onset. $^{***}p \leq .001$.

cardiac acceleration to the US during the first ($t(20) = -8.68$, $p < .001$), second ($t(20) = -7.42$, $p < .001$), and third ($t(20) = -8.08$, $p < .001$) acquisition training. Electrodermal (see Fig. 2B) and cardiac (see Fig. 2C) unconditioned responses did not habituate and were similar for each of the three CS sets (no repeated-measures effects of *Set*, all $ps \geq .554$).

3.2. Subjective ratings and peripheral physiological data during fear extinction

The *Contingency* x *Set* x *Time* ANOVAs for subjective CS ratings during the extinction stage revealed significant *Contingency* x *Time* interactions for valence ($F(3,60) = 48.45$, $p < .001$), arousal ($F(3,60) = 49.52$, $p < .001$), and US expectancy ($F(3,60) = 59.58$, $p < .001$) ratings, indicating successful extinction learning for each CS set (see Fig. 3A). Although differences between CS+ and CS- were not completely absent at the end of extinction training, differential fear responses diminished in each of the three CS sets. Analyses of CS-evoked SCRs ($F(10,200) = 4.26$, $p = .002$) and heart period changes ($F(10,200) = 2.56$, $p = .006$) yielded significant *Contingency* x *Time* x *Set* interactions, reflecting extinction learning (decline of conditioned responses across trials) and habituation (decline across CS sets). As intended, the transition to trials of a new CS set induced "dishabituation", and we observed a successful fear recall during early extinction training for each CS set. Specifically, SCRs (see Fig. 3B) were elevated for CS+ compared with CS- during the first four extinction training trials for CS set 1 ($t(20) = 5.68$, $p < .001$), set 2 ($t(20) = 3.90$, $p = .001$), and set 3 ($t(20) = 2.27$, $p = .035$). Likewise, CS+ versus CS- was associated with cardiac deceleration (see Fig. 3C) during the first four extinction training trials for CS set 1 ($t(20) = 2.22$, $p = .038$), set 2 ($t(20) = 3.62$, $p = .002$), and set 3 ($t(20) = 2.28$, $p = .034$).

3.3. EEG: ERP components during fear acquisition

For day 1 fear conditioning, the TANOVA identified three time windows with continuously significant differences between ERP maps for CS+ and CS- (see Fig. 4A): (a) 33–60 ms[1] (b) 108–200 ms, and (c) 468–820 ms after CS onset. Supporting its validity, our data-driven approach tapped into latencies that overlap with periods reported in previous fear conditioning studies with "traditional" EEG methods (Miskovic and Keil, 2012; Panitz et al., 2015, 2018). A second TANOVA on the amplitude-normalized maps (see Supplementary Material C) indicated that different intracranial brain generators contributed to the effects in each of the three time windows (see Supplementary Fig. S3).

33–60 ms post-CS. As indicated in Fig. 4A, the TANOVA for conditioning revealed significant differences between ERP maps following CS+ versus CS- as early as 33 to 60 ms after stimulus onset (averaged across the significant time window: TANOVA $p = .006$). The grand-grand average ERP (across CS+ and CS- trials and stimulus sets) showed a widespread negativity at centro-parietal electrode sites, in particular at channels CP1, CPz, CP2, P1, Pz, P2, and POz. Thus, mean voltages at these channels were used to compute a *Contingency* x *Set* x *Channel* follow-up ANOVA. A significant *Contingency* main effect ($F(1,20) = 4.70$, $p = .042$) confirmed more negative ERP amplitudes for CS+ compared with CS- (see Fig. 4B). Separate *Contingency* x *Channel* ANOVAs for each of the three CS sets did not reach significance (all $ps \geq .102$). This outcome mirrors previous findings that fear conditioning effects on short-latency sensory processing require a massive number of acquisition trials to be detected (Stolarova et al., 2006; Miskovic and Keil, 2012; Thigpen et al., 2017).

108–200 ms post-CS. The TANOVA further revealed significant differences between CS+ and CS- maps from 108 to 200 ms after stimulus onset (averaged across the significant time window: TANOVA $p < .001$, see Fig. 4A), which survived the duration threshold. This time window comprises a relatively long period, containing a short positive deflection and followed by a more sustained negative deflection. This response pattern was particularly pronounced over occipito-temporal electrode sites. A follow-up ANOVA was conducted at occipito-temporal channels over the left (T7, C5, TP7, CP5, P7, P5, PO7, PO3) and right (T8, C6, TP8, CP6, P8, P6, PO8, PO4) hemisphere. Including the factor *Hemisphere* allowed us to control for lateralization (Caharel et al., 2009; Rossion and Jacques, 2012). This *Contingency* x *Set* x *Channel* x *Hemisphere* ANOVA yielded a significant *Contingency* main effect ($F(1,20) = 23.91$, $p < .001$) and a significant *Contingency* x *Channel* interaction ($F(7,140) = 10.17$, $p < .001$). The effects were comparable across CS sets and hemispheres (ps for interactions $\geq .266$). To further assess the significant interaction with the factor *Channel*, paired-samples *t*-tests were computed for individual EEG channels and indicated a more negative ERP amplitude for CS+ compared with CS- at CP5 ($p = .008$), P7 ($p < .001$), P5 ($p < .001$), PO7 ($p = .001$), and PO3 ($p = .001$) over the left hemisphere, as well as at P8 ($p = .014$), P6 ($p < .001$), PO8 ($p < .001$), and PO4 ($p < .001$) over the right hemisphere (see Fig. 4C). In addition, we computed follow-up *Contingency* x *Channel* x *Hemisphere* ANOVAs for individual CS sets (see Fig. 5A). For the first CS set, a significant *Contingency* main effect ($F(1,20) = 6.06$, $p = .023$) and a significant *Contingency* x *Channel* interaction ($F(7,140) = 3.76$, $p = .030$) confirmed more negative amplitudes for CS+ versus CS-, particularly at parietal and parieto-occipital channels. Likewise, the ANOVA for the second CS set yielded a significant *Contingency* main effect ($F(1,20) = 10.66$, $p = .004$) and a significant *Contingency* x *Channel* interaction ($F(7,140) = 4.99$ $p = .016$). Finally, there was a significant *Contingency* main effect for the third CS set ($F(1,20) = 4.72$, $p = .042$). In summary, our data emphasize the acquisition of a robust conditioned electrocortical response during this period for each of the three CS sets.

468–820 ms post-CS. Finally, the TANOVA showed that CS+ and CS- maps significantly differed from 468 to 820 ms after stimulus onset (averaged across the significant time window: TANOVA $p < .001$, see Fig. 4A), which also survived the duration threshold for overall significance. During this period, the grand-grand average ERP showed strong and sustained positivity at parieto-occipital electrode sites. For follow-up statistical analyses, parieto-occipital channels P1, Pz, P2, PO3, POz, PO4, O1, Oz, and O2 were used, where the late positive voltage deflection was maximal. The follow-up ANOVA including the factors *Contingency* x *Set* x *Channel* revealed a significant *Contingency* main effect ($F(1,20) = 15.24$, $p = .001$), indicating a larger positive deflection for CS+ compared with CS-, as shown in Fig. 4D. Paired-samples *t*-tests confirmed significant effects for all individual EEG channels that were included in the ANOVA. ERP effects in this time window were comparable across CS sets (ps for interactions $\geq .129$). Furthermore, to explicitly confirm ERP modulations for all stimulus sets, separate follow-up *Contingency* x *Channel* ANOVAs for individual CS sets were carried out (see Fig. 5B). We confirmed a significantly larger positive deflection for CS+ compared with CS- for CS set 1 (*Contingency* x *Channel* interaction, $F(8,160) = 2.58$, $p = .044$), set 2 (*Contingency* main effect, $F(1,20) = 16.75$, $p = .001$), and set 3 (*Contingency* main effect, $F(1,20) = 6.22$, $p = .021$).

ERPs evoked by the US. During acquisition training, the US was associated with a robust negative deflection from 50 to 200 ms (see Fig. 6A), followed by a positive deflection from 200 to 350 ms after stimulus onset (see Fig. 6B). The initial negativity was largest at fronto-central channels FC1, FCz, FC2, C1, Cz, and C2 (see Fig. 6C). A *Channel* x *Set* ANOVA

[1] Although this period did not exceed the more conservative duration criterion, previous literature (e.g., Stolarova et al., 2006; Hintze et al., 2014; Mueller and Pizzagalli, 2016; Thigpen et al., 2017) leads us to reasonably expect that fear conditioning modulates such rapid short-lasting neural responses. For TANOVAs, it has been recommended that global duration statistics (indicating "overall" significance) should be treated as "overly conservative in light of pre-existing knowledge about the functional correlates of certain analysis periods" (Habermann et al., 2018). With regard to early-latency ERP modulations (as the present effect), which tend to be of a shorter duration, global duration statistics are particularly conservative. During 33–60 ms, the TANOVA showed a significant difference between CS+ and CS- topographies that did not exceed the more conservative overall duration threshold of 56.64 ms.

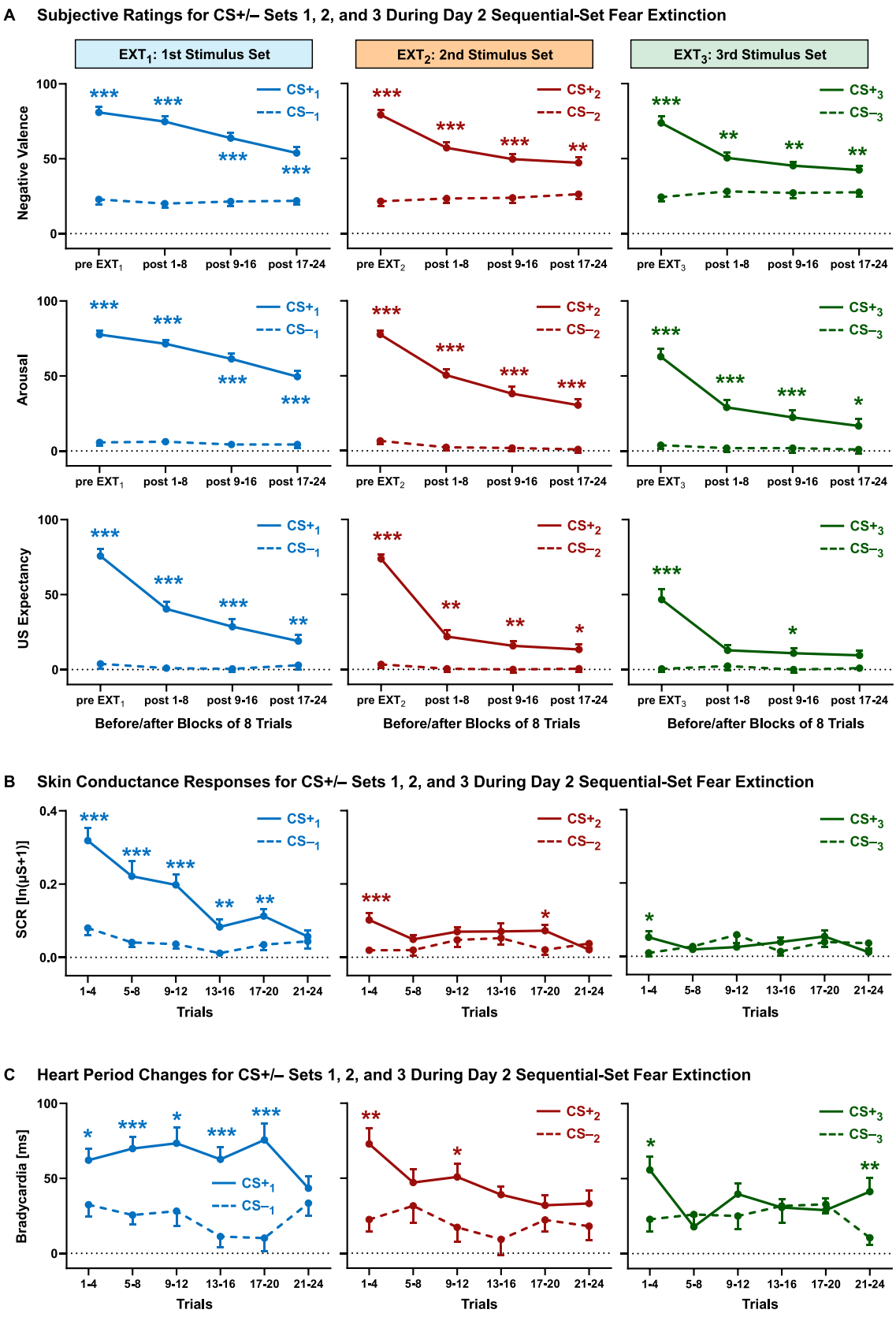

Fig. 3. Subjective and peripheral physiological (electrodermal activity and electrocardiogram) correlates of day 2 sequential-set fear extinction. Conditioned responses are plotted for (A) ratings of CS-associated valence (0 = "very good", 100 = "very bad"), arousal (0 = "not aroused at all", 100 = "extremely aroused"), and US expectancy (0% = "US will definitely not coterminate", 100% = "US will definitely coterminate"), (B) CS-evoked SCR amplitudes, and (C) CS-related heart period slowing (fear bradycardia). Conditioned responses are shown separately for the three CS sets (e.g., $CS+_1$ versus $CS-_1$). Subjective ratings were collected *before* each extinction training phase and *after* blocks of eight trials each. Blocks for peripheral physiological data consisted of four trials each. Line charts display mean values ± within-subject standard errors of the mean (*SEM*, O'Brien and Cousineau, 2014). $^{***}p \leq .001$, $^{**}p \leq .01$, $^{*}p \leq .05$.

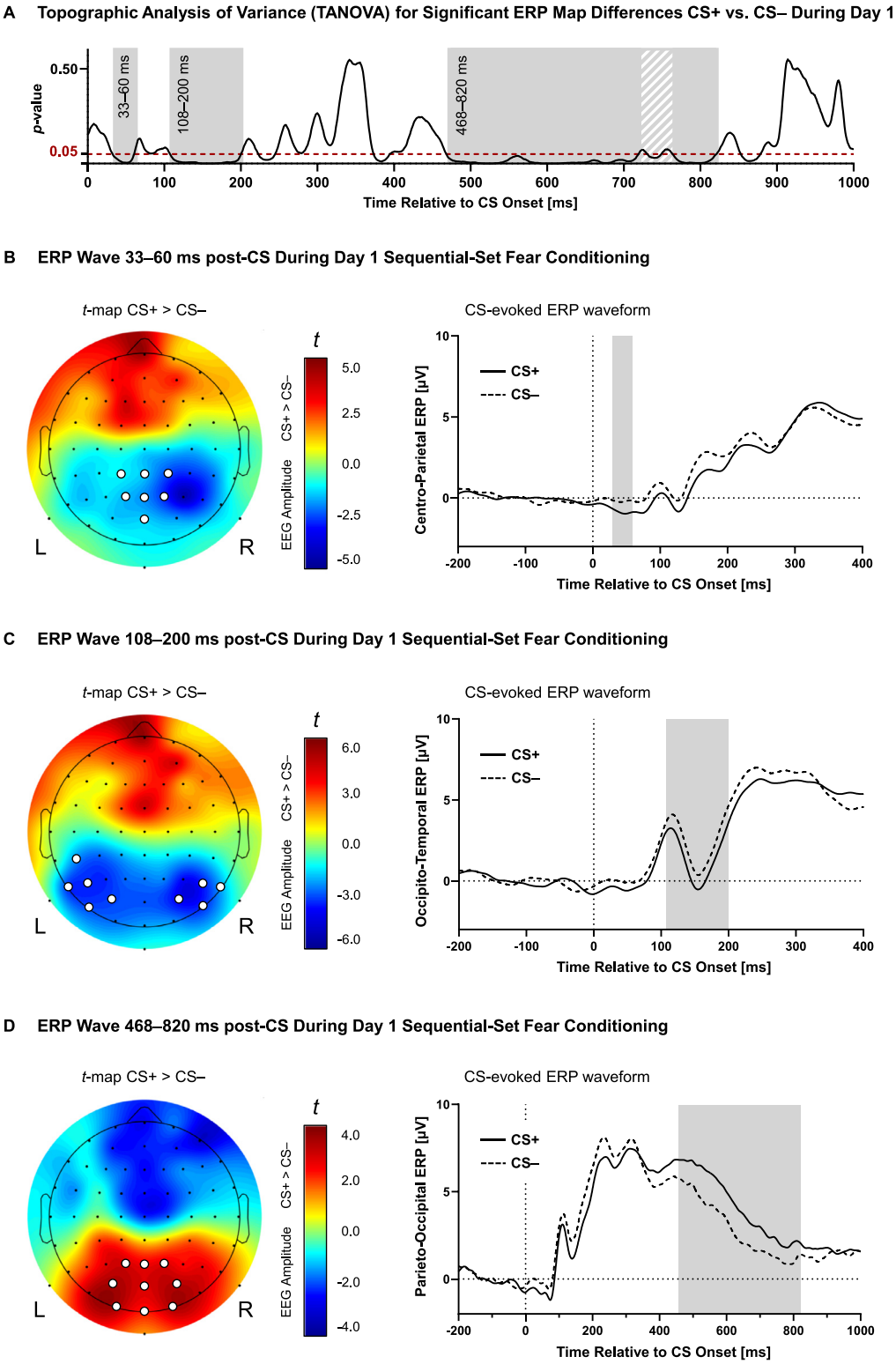

Fig. 4. Event-related potential (ERP) responses evoked by CS+ compared with CS- during day 1 sequential-set fear conditioning. (A) The topographic analysis of variance (TANOVA) indicated that topographic maps were significantly different for CS+ compared with CS- during the 33–60 ms, 108–200 ms, and 468–820 ms periods (i.e., *ps* ≤ .05, gray-shaded area). The last time window was interrupted by a short period (719–730 ms) with .05 ≤ *p* ≤ .08 (shaded in gray and white). (B) During 33–60 ms, the ERP amplitude was significantly more negative for CS+ compared with CS- at centro-parietal electrode sites (left panel). To visualize ERP waveforms (right panel), the electrode sites CP1, CPz, CP2, P1, Pz, P2, and POz were averaged (channels are shown as white dots in the *t*-map). (C) During 108–200 ms, the ERP amplitude was significantly more negative at occipito-temporal channels for CS+ versus CS-. The ANOVA on occipito-temporal ERP amplitudes yielded a significant *Contingency* x *Channel* interaction, and significantly more negative amplitudes for CS+ compared with CS- occurred at CP5, P7, P5, PO7, and PO3 over the left hemisphere, as well as at P8, P6, PO8, and PO4 over the right hemisphere (channels are shown as white dots in the *t*-map). To visualize ERP waveforms (right panel), electrodes with significant effects were averaged. (D) During 468–820 ms, the ERP amplitude was significantly more positive at parieto-occipital channels for CS+ versus CS- (left panel). To visualize ERP waveforms (right panel), the electrode sites P1, Pz, P2, PO3, POz, PO4, O1, Oz, and O2 were averaged (channels are shown as white dots in the *t*-map, significant effects could be confirmed at all electrode sites). The gray-shaded areas in panels B, C, and D indicate the measurement windows for ERP amplitudes. "L" = left hemisphere, "R" = right hemisphere. Note: A schematic illustration of the EEG montage with electrode labels is available at https://doi.org/10.5281/zenodo.4294603.

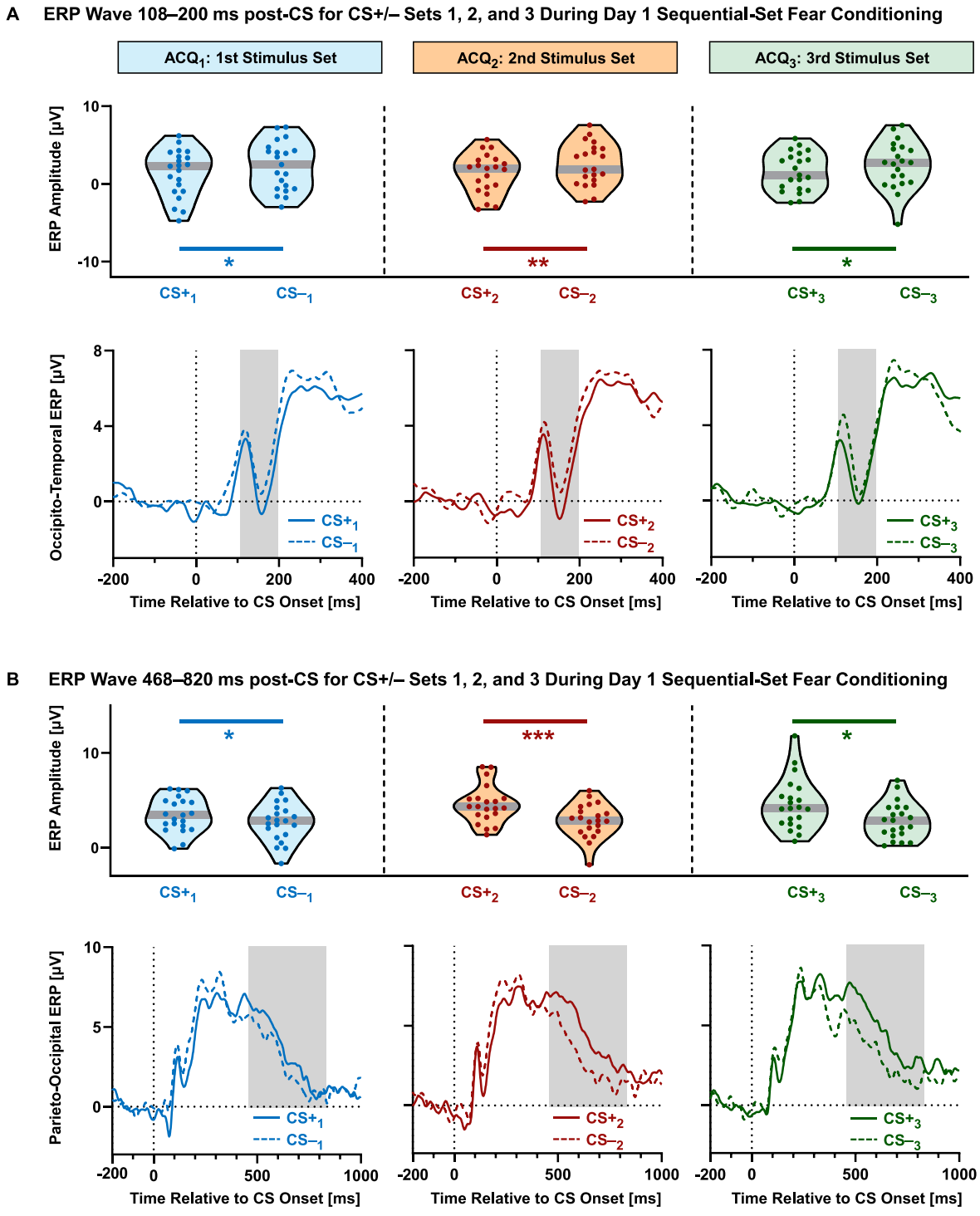

Fig. 5. Event-related potential (ERP) responses evoked by CS+ compared with CS- during day 1 sequential-set fear conditioning were comparable across the three stimulus sets. (A) The ERP amplitude during 108–200 ms after CS onset was significantly more negative for CS+ compared with CS- in all three CS sets. The *Contingency* x *Set* x *Channel* x *Hemisphere* ANOVA yielded a significant *Contingency* x *Channel* interaction, and the ERP amplitudes were significantly more negative for CS+ compared with CS- at CP5, P7, P5, PO7, and PO3 over the left hemisphere, as well as at P8, P6, PO8, and PO4 over the right hemisphere. To visualize ERP waveforms during this period, electrodes with significant effects were averaged. (B) The ERP amplitude during 468–820 ms time-locked to the CS onset was significantly more positive for CS+ compared with CS- in all three CS sets. To visualize ERP waveforms, the parieto-occipital electrode sites P1, Pz, P2, PO3, POz, PO4, O1, Oz, and O2 were averaged (significant effects could be confirmed at all electrode sites). In the upper panels, violin plots display the frequency distribution of the ERP data. Individual data points are superimposed on the violin plot, and the median is displayed as a grey horizontal line. In the lower panels, the time series of CS-evoked changes in voltage (relative to baseline) are shown. Gray-shaded areas indicate time windows for statistical analyses. $^{***}p \leq .001$, $^{**}p \leq .01$, $^{*}p \leq .05$.

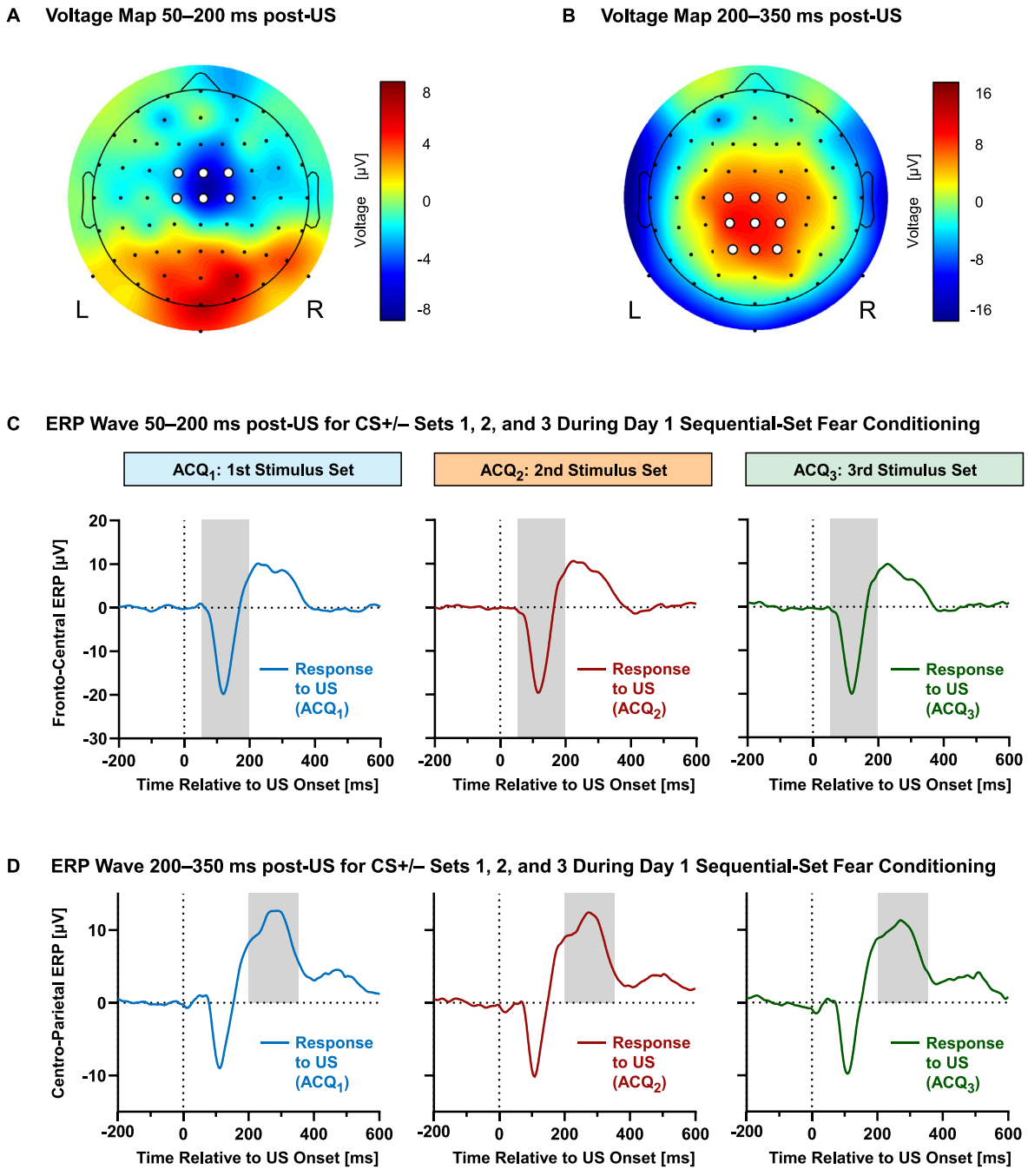

Fig. 6. Event-related potential (ERP) responses evoked by the US during day 1 sequential-set fear conditioning were comparable across the three acquisition training phases for CS set 1, set 2, and set 3. The US was associated (A) with a large fronto-central negative deflection from 50 to 200 ms, followed by a (B) centro-parietal positive deflection from 200 to 350 ms after stimulus onset (gray-shaded areas). (C) To visualize ERP waveforms during the 50–200 ms period, the electrode sites FC1, FCz, FC2, C1, Cz, and C2 were averaged (channels are shown as white dots in the voltage map). (D) To visualize ERP waveforms during the 200–350 ms period, the electrode sites C1, Cz, C2, CP1, CPz, CP2, P1, Pz, and P2 were averaged (channels are shown as white dots in the voltage map). "L" = left hemisphere, "R" = right hemisphere. Note: A schematic illustration of the EEG montage with electrode labels is available at https://doi.org/10.5281/zenodo.4294603.

showed a significant main effect of *Channel* ($F(5,100) = 8.27$, $p < .001$). Effects were most substantial at midline channels, and extended mainly to channels over the right hemisphere (see Fig. 6A), consistent with previous research indicating enhanced amplitudes during this period over channels *contralateral* to the hand receiving electric shocks (Wang et al., 2014). Conversely, during the 200–350 ms period, we observed a reliable positive deflection (see Fig. 6D) at centro-parietal channels C1, Cz, C2, CP1, CPz, CP2, P1, Pz, and P2. Unconditioned responses during both time windows did not habituate and were similar across CS sets (no repeated-measures effects of *Set*, all $ps \geq .179$)

Collectively, ERP analyses revealed that fear conditioning was accompanied by enhanced EEG amplitudes for CS+ compared with CS- during three distinct time windows. Conditioned responses were similar across all three CS+/CS- sets. To calculate effect sizes for ANOVA main effects, the mean values for CS+ and CS- were computed (averaged across other ANOVA factors). According to Cohen's (1988, 1992) benchmark, participants learned a *large* electrocortical fear response (CS+ versus CS-) for the 108–200 ms ($d = 1.11$) and 468–820 ms ($d = 0.85$) time windows, whereas they acquired a *medium to large* effect for the 33–60 ms period ($d = 0.47$).

3.4. EEG: ERP components during fear extinction

For day 2 fear extinction, the TANOVA (see Supplementary Material D) indicated significant differences between ERP maps for CS+ and CS- in the time window from 460 to 730 ms after CS onset (averaged across the significant time window: TANOVA $p < .001$). An additional TANOVA on the amplitude-normalized maps confirmed that, similar to effects during the acquisition stage, different intracranial brain generators were involved (see Supplementary Fig. S4). In earlier time windows, the TANOVA did not reach significance and topographies for CS+ and CS- were comparable.

460–730 ms post-CS. This time window is very similar to the late-latency period we observed during day 1 fear conditioning. The topography of the grand-grand average ERP converged with results from day 1, and we observed a sustained positive deflection at parieto-occipital electrode sites. Emphasizing the robustness and validity of the conditioned fear response, the TANOVA for the extinction stage suggested that late-latency conditioning effects, which have already been reported during day 1, remained significant 24 h later. We computed a *Contingency* x *Set* x *Channel* x *Time* ANOVA at parieto-occipital channels P1, Pz, P2, PO3, POz, PO4, O1, Oz, and O2. This analysis confirmed that CS+ evoked a larger positivity compared with CS- (*Contingency* main effect, $F(1,20) = 22.50$, $p < .001$). As expected, a trendwise *Contingency* x *Time* interaction ($F(2,40) = 2.97$, $p = .063$) indicated that the differential fear response declined from early to late extinction training, a phenomenon that supports the formation of a new extinction memory trace. For all individual EEG channels included in the ANOVA, paired-samples *t*-tests confirmed significant effects. Importantly, these late ERP effects during extinction were comparable across CS sets, and follow-up ANOVAs for individual sets confirmed significant *Contingency* main effects for CS set 1 ($F(1,20) = 16.36$, $p = .001$), set 2 ($F(1,20) = 11.33$, $p = .003$), and set 3 ($F(1,20) = 14.33$, $p = .001$). Accordingly, slow-wave conditioning effects remained significant 24 h after fear conditioning.

3.5. EEG: learning dynamics of ERP effects as revealed by block-wise analyses after averaging across CS sets

Due to the relatively low signal-to-noise ratio of EEG signals, averaging across a large number of trials is necessary to detect ERP signatures of fear conditioning (Miskovic and Keil, 2012; Steinberg et al., 2013; Huffmeijer et al., 2014). However, such aggregations will wash out temporal changes in neural responding over time (Ferreira de Sá et al., 2019). In fact, given that the subjective expectancy regarding the CS-US contingency is changing throughout learning, we assume that neural fear responses are not stable across all trials. Instead, differential conditioned responses rise from early to late conditioning and decline from early to late extinction learning. This fact has often been ignored in conventional EEG studies (Miskovic and Keil, 2012). In contrast, *sequential-set* conditioning allows us to average across CS sets at specific time points in the conditioning stage, creating the possibility to tap into more transient neurophysiological processes and to detect *temporal changes* during learning with a sufficient signal-to-noise ratio.

To detect changes over time, the acquisition training phases were split into three sub-blocks of five trials each. In a similar way, the extinction training phases were split into six sub-blocks of four trials each. To control for EEG responses before conditioning, the four pre-acquisition trials were also averaged. Despite averaging only a small number of trials within each stimulus set (e.g., five trials during conditioning), averaging across all three CS sets triples the number of trials. As reported above, the acquisition ANOVA for the 108–200 ms period yielded a significant *Contingency* x *Channel* interaction, while statistical analyses for the 33–60 ms and 468–820 ms periods showed comparable effects for all channels included in the ANOVAs. To analyze temporal changes during learning, electrodes with significant effects were averaged. Importantly, these analyses on learning dynamics of EEG effects revealed a linear growth of electrocortical fear responses from early to late conditioning.

Differential EEG responses during 33–60 ms after CS onset increased throughout fear acquisition trials, as indicated in Fig. 7A. Specifically, a polynomial trend analysis showed that differential fear responses followed a linear growth curve (linear trend for the *Contingency* x *Sub-Block* interaction: $F(1,20) = 7.33$, $p = .014$). There was no difference during pre-acquisition ($t(20) = 0.90$, $p = .381$), but ERP responses were significantly larger (i.e., more negative) during the last five acquisition training trials ($t(20) = -3.70$, $p = .001$). Likewise, effect sizes increased step by step (see blue bars in Fig. 7A), and we observed a large effect ($d = 0.81$) toward the end of conditioning.

There was a similar pattern 108–200 ms after CS onset (see Fig. 7B). Differential fear responses increased from early to late conditioning (linear trend for the *Contingency* x *Sub-Block* interaction: $F(1,20) = 9.60$, $p = .006$). During the pre-acquisition trials, there was no difference between ERP responses to CS+ and CS- ($t(20) = 1.60$, $p = .126$). Conversely, CS+ compared with CS- evoked a significantly larger negativity during the last four acquisition trials ($t(20) = -3.12$, $p = .005$). Effect sizes showed a sharp rise during the first five acquisition training trials and reached a plateau with notably smaller subsequent changes (see blue bars in Fig. 7B).

Finally, conditioned fear responses during the 468–820 ms post-CS period (see Fig. 7C and E) also followed a linear learning curve, and polynomial analyses confirmed a linear trend for the *Contingency* x *Sub-Block* interaction ($F(1,20) = 21.64$, $p < .001$). While CS-evoked ERPs were comparable during the pre-acquisition trials ($t(20) = -1.08$, $p = .294$), CS+ versus CS- led to a significantly stronger positivity toward the end of acquisition training ($t(20) = 3.68$, $p = .001$). Effect sizes constantly increased during fear conditioning (see blue bars in Fig. 7C).

Twenty-four hours later, no effects could be detected for short- and mid-latency ERPs (see Supplementary Material E), suggesting that sensory processing was similar for CS+ and CS-. However, differential fear responses in the late-latency period from 460 to 730 ms (see Fig. 7D and F) gradually diminished from early to late extinction learning (linear trend for the *Contingency* x *Sub-Block* interaction: $F(1,20) = 8.80$, $p = .008$). Specifically, CS+ compared with CS- evoked a significantly larger positivity during the first four extinction training trials ($t(20) = 4.64$, $p < .001$). Differential fear responses vanished toward the end of extinction training ($t(20) = 0.93$, $p = .362$). Similarly, effect sizes successively declined from trial to trial during extinction training (see blue bars in Fig. 7D).

4. Discussion

Fear conditioning and extinction describe learning processes during which fear responses *increase* and *decrease* over time, respectively. The overarching goal of this study was to reconstruct the learning curves of neural processes during fear conditioning and extinction in humans. To date, several studies have investigated ERPs during fear conditioning (Miskovic and Keil, 2012), but little is known about how electrocortical signatures gradually evolve from trial to trial. The relatively poor signal-to-noise ratio of EEG recordings requires averaging across a high number of trials, a factor that impedes the analysis of fear learning from one moment to another (Steinberg et al., 2013; Huffmeijer et al., 2014). However, the informational value of CS+ and CS-, which is critical for learning, is changing during learning (Rescorla and Wagner, 1972; Tzovara et al., 2018) because the associative strength between CS+ and the US is gradually increasing (conditioning) or decreasing (extinction). Neurophysiological processes that are responsible for the initial acquisition of CS-US contingencies show a fast habituation pattern over time (Yin et al., 2018). Thus, neural responses that are specific for the formation of fear memories are particularly pronounced during early learning phases (Büchel et al., 1998; LaBar et al., 1998). Accordingly, neurophysiological indices of fear are supposed to change across trials due to learning (i.e., due to changes in associative strength) and habituation (i.e., due to repeated stimulation). A suitable paradigm that allows one to investigate neural dynamics of fear learning has been missing so far.

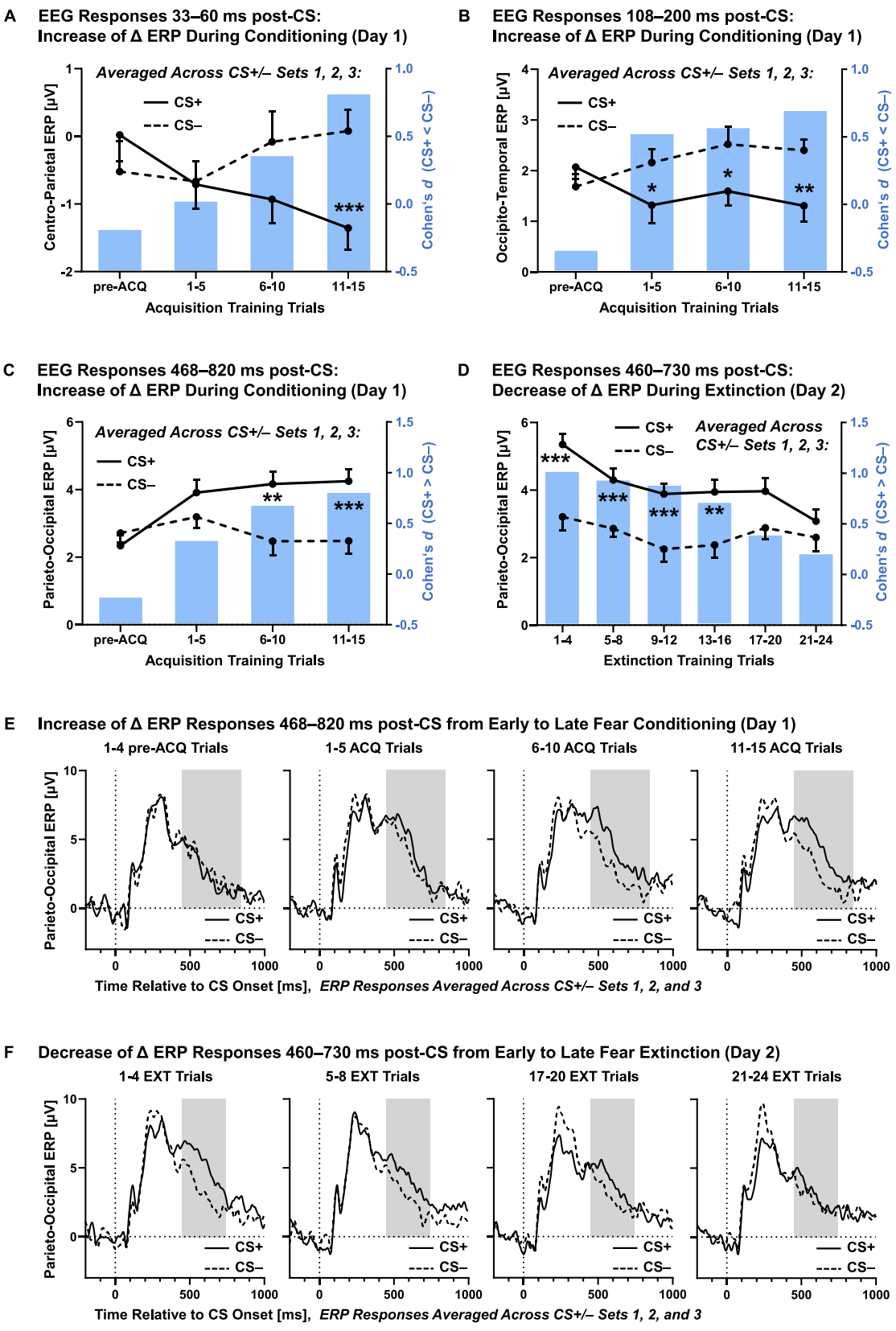

Fig. 7. To detect changes over time, the acquisition and extinction training phases were split into smaller sub-blocks of five (acquisition) or four (pre-acquisition and extinction) trials each. Averaging across trials from all three conditioned stimulus (CS+/CS-) sets allows studying the increase and decrease of Δ ERPs (CS+ versus CS-) during fear conditioning and extinction, respectively. Conditioned EEG responses during the (A) 33–60 ms, (B) 108–200 ms, and (C, E) 468–820 ms periods increased from early to late fear conditioning (day 1). Conversely, conditioned responses during (D, F) 460–730 ms decreased from early to late extinction (day 2). Line charts (A–D) show the mean voltage for CS+ and CS- for each sub-block (± within-subject *SEM*, O'Brien and Cousineau, 2014). Blue bars indicate how effect sizes (Cohen's *d*, plotted on the right y-axis) for conditioned electrocortical responses increased during fear conditioning (A–C) and decreased during fear extinction (D). $^{***}p \leq .001$, $^{**}p \leq .01$, $^{*}p \leq .05$.

Here, we fill this gap by providing evidence about transient changes in EEG responses during fear conditioning and extinction using a new *sequential-set* fear conditioning paradigm. To minimize attenuation of fear responses across trials, fear conditioning and extinction consist of three successive phases. For each phase, a novel CS+/CS- set is used. Importantly, changes in neural responding between smaller subsets of trials emerge after averaging across CS sets.

During fear conditioning, all reported measures pointed toward a similarly strong conditioned response for CS sets 1, 2, and 3. Consistent with prior research (Bradley et al., 2005; Castegnetti et al., 2016; Marin et al., 2020), CS+ versus CS- evoked elevated skin conductance responses and relative fear bradycardia, reflecting heightened physiological arousal and vigilance in anticipation of the US (Davis and Lang, 2003; Löw et al., 2015). Peripheral physiological responses to the CS+ may thus be interpreted as an indicator that on-going behavior was interrupted and attention was oriented toward the threat cues (Blanchard et al., 2011), which can be critical for survival (Mobbs et al., 2015). On the subjective level, CS+ compared with CS- was associated with higher ratings of negative valence, arousal, and US expectancy. Concerning EEG data, we did not have any *a priori* constraints and applied a *data-driven* approach to identify ERP components that are modulated by fear learning. Demonstrating the suitability of our paradigm to assess EEG responses to threat, we captured short-, mid-, and long-latency electrocortical processes. Specifically, CS+ compared with CS- elicited elevated ERP amplitudes during the 33–60 ms, 108–200 ms, and 468–820 ms periods. Our results suggest preferential and facilitated processing of aversive cues during various stages. Consistent with the conceptualization of a "threat sensitization" hypothesis (Bublatzky and Schupp, 2012), fear conditioning seems to prioritize neural transmission and enhance selective attention toward signals of danger. Notably, after averaging across CS sets, we were able to reconstruct learning curves for ERPs in these periods.

It is important to point out that relevant time windows for ERP analyses were derived from a data-driven approach. In contrast, ERP *components* are usually defined based on distinct electrophysiological properties (latency, polarity, amplitude, topography). ERP components are often conceptualized as peaks in the observed scalp waveform. However, this practice can be problematic, as underlying "latent" components may differ (Luck, 2014). Underlying components are considered to be neural processes which sum together and produce an ERP wave that can be measured with electrodes on the scalp (Luck and Kappenman, 2019). Though, it is important to remember that multiple underlying components mix in the scalp ERP waveform, which are difficult to disentangle. If an ERP component is quantified based on a pre-defined measurement window, it is most likely that EEG activity during this period is related to multiple underlying "latent" components. In addition, important effects may be missed if the analysis is limited to specific periods. Here, we circumvented this problem and used a data-driven approach to isolate time windows that are relevant for fear conditioning and extinction. Specifically, we computed a TANOVA and explored during which periods ERPs evoked by the CS+ and CS- differed in response strength and topography. Compared with "traditional" ERP analyses, this approach is much more flexible and powerful, as all electrodes and time frames are considered. There is no simple or one-to-one mapping between TANOVA-derived periods and "traditionally" defined ERP waves. Nevertheless, effects may overlap partly. In order to link our findings with the previous fear conditioning literature, it is helpful to speculate which ERP components might be involved during the time windows reported in the present study. Sketching out relationships between specific ERP periods and different brain functions allows to draw inference about how threatening cues guide attention and processing speed (Bublatzky et al., 2010; Bublatzky and Schupp, 2012; MacNamara et al., 2013; Klumpp and Shankman, 2018).

First, we found a more negative ERP amplitude to CS+ versus CS- as early as 33–60 ms after CS onset, suggesting rapid detection of fear-conditioned stimuli and privileged signal transmission during the earliest processing stages. Some previous EEG studies demonstrated that fear conditioning can modulate already early processing in visual cortices (Stolarova et al., 2006; Hintze et al., 2014; Mueller and Pizzagalli, 2016; Thigpen et al., 2017). Mirroring the results of our data-driven approach, amplified neural responses to visual fear-conditioned stimuli have been reported as early as 30–60 ms (Morel et al., 2012), 41–55 ms (Mueller and Pizzagalli, 2016), and 50–80 ms (Steinberg et al., 2012, 2013). Subcortical brain regions may be closely linked with perceptual areas (Freese and Amaral, 2005; Chen et al., 2009; Pourtois et al., 2013) and initially gate threat processing in visual regions (Vuilleumier et al., 2004; Rotshtein et al., 2010). Research in macaque monkeys revealed a substantial modulatory control of amygdaloid projections over processing in sensory pathways (Amaral et al., 2003), which may thereby boost early brain responses to emotional information (Vuilleumier, 2009). Over the course of learning, plastic changes in primary visual cortex neurons may further lead to a facilitated perception of threat stimuli (Keil et al., 2007; McTeague et al., 2015; Thigpen et al., 2017). Sparsification of neural representations as well as enhanced synaptic efficiency may explain this successive shift in processing toward neurons with shorter response latencies (Stegmann et al., 2020; Wieser and Keil, 2020). This interpretation is in line with the idea that fear memory formation initially involves a widespread neural network, which may be sharpened across learning trials to involve more specialized neurons in sensory regions (Moratti et al., 2006; Miskovic and Keil, 2012; Thigpen et al., 2017). Crucially, the learning curve of the 33–60 ms effects in our data closely mirrors this hypothesis of subsequent visual cortex plasticity: While there was no significant difference in ERP responses to CS+ and CS- during early conditioning, we observed a large differential fear response only during the last five conditioning trials. After repeated learning experiences, short-term plasticity may promote biased perception even in early regions of the visual hierarchy, which have not been considered to be sensitive for attentional modulations in traditional models (Gomez Gonzalez et al., 1994; Clark and Hillyard, 1996; Anderson, 2011). Linking this effect to "classical" ERP components is challenging. The C1 wave is considered to be one of the earliest visual ERP components and is thought to be generated mainly in the primary visual cortex (Jeffreys and Axford, 1972; Clark et al., 1994; Rauss et al., 2011). The C1 wave typically starts 40–60 ms and peaks 80–100 ms after stimulus onset (Luck, 2014). In the present study, we found an effect beginning at 33 ms already, which is earlier compared to genuine C1 waves described in the literature. However, animal studies report that the earliest visual response latencies in the macaque primary visual cortex start around 35 ms after stimulus onset (Lamme and Roelfsema, 2000). Using intracerebral ERP recordings in epileptic patients, Kirchner et al. (2009) demonstrated that sensory characteristics of visual stimuli can modulate neural activity during ultra-rapid latencies between 45 and 60 ms after stimulus onset. Furthermore, electromagnetic studies in humans suggest discriminative processing of face stimuli during very early latencies of 30–60 ms (Braeutigam et al., 2001) and 40–50 ms (Morel et al., 2009). Responses to non-face stimuli were weaker and less widespread (Braeutigam et al., 2001), suggesting that a fast detection of face stimuli has been of particular relevance in the evolutionary past (Kret and Gelder, 2012). Our findings emphasize that fear conditioning can boost the earliest stages of visual processing, which may either be related to subcortical projections or – during later trials – reflect an ultra-rapid feed-forward flow of sensory information (Pourtois et al., 2013; Thigpen et al., 2017).

Second, fear conditioning was associated with potentiated ERP amplitudes between 108 and 200 ms after CS onset, which may reflect privileged sensory processing of threat in extrastriate regions (Clark and Hillyard, 1996; Linkenkaer-Hansen et al., 1998). This is a relatively broad time window, which includes the typical latencies of the P1 and N170 ERP components (Desjardins and Segalowitz, 2013). During this period, CS+ versus CS- faces evoked more negative amplitudes at occipito-temporal channels, corresponding to the typical scalp distribution of these components (Eimer, 2011; Rossion and Jacques, 2012;

Luck, 2014). Remarkably, our results also demonstrate the temporal evolution of fear conditioning effects during the 108–200 ms period: We observed a significantly more negative ERP amplitude for CS+ compared with CS- already during the first five conditioning trials, while differential effects remained stable and slightly increased over the subsequent course of conditioning. Rotshtein et al. (2010) reported that amygdala damage leads to diminished ERPs for fearful faces during 100–150 ms post-stimulus. Considering the crucial role of the amygdalar circuits for fear conditioning (LeDoux, 2014; Janak and Tye, 2015), we can assume that this time window is of particular relevance for rapid threat processing already during early conditioning trials. With regard to the common ERP literature, our observation during the 108–200 ms period may be linked to a combination of attenuated (i.e., less positive) P1 amplitudes and magnified (i.e., more negative) N170 amplitudes. Effects related to these processes are difficult to disentangle with the current experimental design. Liu et al. (2012b) showed decreased P1 amplitudes after CS+ versus CS- for well-trained stimulus pairs. Consistent with the prediction error theory of attention during classical conditioning (Pearce and Hall, 1980), we may speculate that the required level of attention decreases as the US is fully predicted by the CS (Liu et al., 2012b). Changes in US expectancy seem to be critical for learning, especially during *early* fear conditioning trials (Wills, 2009). Supporting our interpretation, ERP and eye tracking studies suggest a correlation between differences in attention and the size of the previously produced prediction error (Wills et al., 2007; Wills, 2009). In addition, similar to our findings, Rigoulot et al. (2008) reported a P1 reduction for unpleasant compared with neutral pictures. Given that we used different face stimuli as CSs, it is important to keep in mind that the 108–200 ms period can also include activity which may be related to the N170 component. This component is particularly enhanced for faces (Eimer, 2011; Schweinberger, 2011; Rossion and Jacques, 2012) and involves face-selective generators (McKone and Robbins, 2011) from the fusiform gyrus (Gao et al., 2019). Larger (i.e., more negative) N170 amplitudes for CS+ compared with CS- may reflect heightened allocation of attentional resources to fear-conditioned faces, due to their high evolutionary significance (Kret and Gelder, 2012). While some studies negated an emotional modulation of the N170 complex (e.g., Eimer et al., 2003; Holmes et al., 2005), others reported larger amplitudes for fearful compared with neutral facial expressions (e.g., Blau et al., 2007; Schindler et al., 2019). Likewise, some electromagnetic fear conditioning studies have reported that faces or face-like stimuli that signal danger elicit changes in brain activity during the N170 period (Pizzagalli et al., 2003; Steinberg et al., 2012; Levita et al., 2015; Camfield et al., 2016; Mueller and Pizzagalli, 2016; Watters et al., 2018).

Third, at 468–820 ms from CS onset, CS+ compared with CS- elicited greater positivity at parieto-occipital EEG channels. The late latency and topographic distribution make us reasonably assume that effects during this period presumably reflect activity of the LPP (Schupp et al., 2006; Hajcak et al., 2018; Hajcak and Foti, 2020). High arousal and motivational salience of emotional stimuli consistently evoke amplified LPP responses, which can persist for hundreds of milliseconds (Schupp et al., 2006; Hajcak et al., 2018) and are generated in an extensive cortical and subcortical network (Liu et al., 2012a). A body of fear conditioning studies (Panitz et al., 2015, 2018; Pastor et al., 2015; Bacigalupo and Luck, 2018; Seligowski et al., 2018; Ferreira de Sá et al., 2019; Pavlov and Kotchoubey, 2019; Stolz et al., 2019) has provided evidence that CS+ evokes larger LPP amplitudes than CS-. Amplified LPP responses for the CS+ can be interpreted as an indicator of stimulus significance (Hajcak and Foti, 2020), reflecting elaborative processing and the activation of a cortico-limbic defensive system (Bradley, 2009). In terms of “motivated attention”, emotionally arousing stimuli activate motivational circuits in the brain which are related to survival behavior (e.g., escape, attack) and require a sustained allocation of attentional resources (Lang et al., 1997; Schupp et al., 2004; Pastor et al., 2008). Extending previous findings, we observed a stepwise increase of slow-wave fear responses during conditioning. Our data indicate that effect sizes accumulated from trial to trial, and a large fear response was acquired toward the end of conditioning. Together, these findings suggest that sustained attention and elaborative processing of the threat-predicting CS+ (Cuthbert et al., 2000; Nelson et al., 2015b; Weinberg et al., 2015) progressively gained during learning. In contrast to mid-latency responses, ERPs from 468 to 820 ms showed a slower increase and were particularly pronounced during late conditioning trials, which may represent functional differences in attentional processes. During later conditioning trials, the uncertainty about the CS-US contingencies gets gradually reduced and the US becomes reliably predicted by the CS+. Thus, the danger is getting more imminent (Davis and Lang, 2003; Lang and Bradley, 2013; Löw et al., 2015), which requires the preparation of defensive threat reactions (Roelofs, 2017). With growing awareness about the CS-US contingency, motivational top-down factors (e.g., emotional evaluation, cognitive reappraisal and regulation strategies, active searching for threat cues) may become more and more important (Olofsson et al., 2008; Hajcak et al., 2010; Mohanty and Sussman, 2013; Myruski et al., 2019).

As discussed above, fear conditioning was accompanied by relatively more negative ERP activity to the CS+ compared with CS- during short- (33–60 ms) and mid-latency (108–200 ms) periods. Moreover, during the late-latency period (468–820 ms), this effect basically swaps, and we observed a more positive amplitude for CS+ versus CS-. Considering this intriguing dynamic across the three time windows, the late-latency effect (468–820 ms) was evident as a sustained positivity across parieto-occipital sites and can thus be reliably interpreted as an indicator of enhanced stimulus significance for the CS+, accompanied by sustained allocation of attentional resources (Hajcak and Foti, 2020). However, the interpretation of the polarity of effects during the short-latency period (33–60 ms) is more challenging. Due to the retinotopic organization of the striate cortex, ERPs within the first 100 ms after stimulus onset can either appear as a negative or positive voltage deflection, depending on whether the stimulus was presented in the upper or lower visual field, respectively (Clark et al., 1994). Here, we observed an early negativity at centro-parietal channels for the CS+, which was almost absent for the CS-. Thus, we believe that this effect represents a larger negativity for CS+ compared with CS-, which can be interpreted as *elevated* sensory processing. However, we cannot fully exclude that this effect might be driven by a reduced positivity for the CS+, which would indicate *attenuated* sensory processing. This alternative explanation could be ruled out in future studies if the location of the CS+ and CS- would explicitly be varied between the upper and lower visual field. During the 108–200 ms period, the voltage was more negative for CS+ versus CS-. This time window comprises a relatively long period, which includes neural processes that may be linked to the P1 and N170 components. Thus, this effect could be related to a reduced positive deflection, to a larger negative deflection, or to a combination of both. On the one hand, as discussed above, an attenuated positivity could indicate that less attention is required if the US is reliably predicted by the CS+ as fear conditioning proceeds, which would be consistent with the P1 literature (Liu et al., 2012b). On the other hand, following the N170 literature, a larger negativity could reflect heightened attentional engagement with fear-conditioned faces (Eimer, 2000, 2018; Schweinberger, 2011). To disentangle both processes, future studies should assess whether effects can be replicated with non-face CSs, which would reduce the influence of processes that are related to the face-sensitive N170 component.

For day 2, the TANOVA on the first extinction training block (i.e., the first 8 trials) revealed a larger positivity for CS+ compared with CS- at parieto-occipital channels between 460 and 730 ms after CS onset. Conditioned responses were similar for extinction phases 1, 2, and 3, underlining the robustness of this slow-wave fear response. The latency and topography of effects during this period converge with the LPP-related time window that we observed during fear conditioning on day 1. As expected, LPP-related effects faded over the course of extinction learning. The decline of this late-latency fear response indicates that less allocation of attentional resources is required when the CS+ faces no longer

predict an aversive outcome. Violating the US expectancy (Craske et al., 2018) seems to be critical for the formation of a new extinction memory trace (Bouton, 2017), which alters the predictive value (Myers and Davis, 2007) and stimulus significance (Hajcak and Foti, 2020) of the CS+. Reduced LPP responses during fear extinction may be related to top-down inhibitory signaling (Pourtois et al., 2013) from prefrontal areas (Adhikari et al., 2015; Jayachandran et al., 2019; Marek et al., 2019), which are crucially involved in extinction learning (Milad and Quirk, 2012). The decrease of late-latency ERP responses was accompanied by diminished electrodermal and cardiac fear indices. Altogether, we assume that extinction learning was presumably associated with a reduction in motivated attention toward the CS+ (Lang et al., 1997; Schupp et al., 2004; Pastor et al., 2008).

Previous fear conditioning studies were primarily interested in amplitude differences between ERPs evoked by CS+ and CS-. Conversely, topographic differences between conditions have often been ignored in EEG research (Michel and Murray, 2012). Here, we used a data-driven TANOVA approach which captures ERP effects that may be related to differences in both amplitude strength (i.e., amount of simultaneously active sources) *and* topography (i.e., location/orientation of active sources). Additional analyses on differences between the amplitude-normalized maps revealed that our ERP effects seem to be partially related to different generator configurations. Notably, Murray et al. (2008) hypothesized that stimuli of negative emotional valence may be processed through a more efficient neural circuit, which would imply the contribution of (at least partially) different generators. This interpretation is consistent with our findings, suggesting that fast and prioritized signaling for fear-conditioned stimuli may, to some extent, involve segregated neural pathways (LeDoux, 1995, 2000).

Because of their high preparedness for fear conditioning, we used faces as CSs (Lissek et al., 2005), which seem to be processed in a rapid and automatic fashion in the human brain (Palermo and Rhodes, 2007; Tamietto and Gelder, 2010). Due to their evolutionary significance, a large amount of studies investigated ERPs to face stimuli in order to uncover attentional processes. In a recent review, Schindler and Bublatzky (2020) synthesize findings on emotional face processing, and point out that the influence of attention and emotion on face perception highly depends on the visual processing stage. The most consistent finding seems to be that attention to fearful faces leads to enhanced P3/LPP amplitudes (Schindler and Bublatzky, 2020), which may be explained by a larger impact of controlled attention (Hajcak et al., 2009) on later processing stages, especially toward potential danger (Schindler et al., 2020). This observation is complemented by our findings, as we detect late-latency fear responses during both fear conditioning and fear extinction stages. In contrast, short- (33–60 ms) and mid-latency (108–200 ms) ERP modulations emerged only during fear conditioning, but not during fear extinction. Mueller and Pizzagalli (2016) reported that remotely fear-conditioned faces can modulate rapid (< 80 ms) processing in visual brain regions even one year after acquisition, suggesting that conditioning effects might have been less stable in the present study. Furthermore, early ERP responses could depend more heavily on the threatening nature of the experimental context (Gelder et al., 2006; Muench et al., 2016), which may differ between conditioning and extinction stages. Moreover, transient and earlier brain processes may primarily be involved in the *acquisition* of emotional memories (Ferreira de Sá et al., 2019), which requires fast adaptation to threat. We assume that fear conditioning recruits a sensory-vigilance network, which is governed by the amygdala and fast projections to sensory cortices (Davis and Whalen, 2001; Sabatinelli et al., 2009; Shackman et al., 2011). Conversely, extinction learning seems to be mediated by top-down controlled influences from the prefrontal cortex (Milad and Quirk, 2012; Adhikari et al., 2015; Marek et al., 2019), which may affect rather late processing stages (Pourtois et al., 2013).

Taken together, we successfully demonstrated that sequential-set conditioning prevents habituation to the CSs, and allows to uncover the learning dynamics of perceptual and attentional processes. In addition to CS-evoked responses, we also assessed unconditioned responses. In a previous study we demonstrated that fear conditioning can be dramatically impaired if the US intensity does not remain high enough throughout acquisition trials (Sperl et al., 2016). To overcome this problem, the electrotactile US was applied in a relatively high shock intensity compared with the majority of fear conditioning studies (Sehlmeyer et al., 2009; Lonsdorf et al., 2017). As intended, peripheral and central physiological responses to the US resisted habituation. We observed a similarly strong unconditioned response during the acquisition trainings of CS set 1, set 2, and set 3. On the peripheral physiological level, the US evoked robust SCRs and cardiac acceleration, supporting fight-or-flight behavior. Replicating previous findings, we demonstrated that the US evoked an accelerative response (Ginsberg and Thysell, 1966; Lipp and Vaitl, 1990; Vila et al., 2007; Mueller et al., 2019), while the CS+ (as discussed above) was associated with relative heart rate deceleration. At first glance, this divergence between autonomic unconditioned and conditioned responses may seem paradoxical. However, the relative dominance of sympathetically driven acceleration and parasympathetically dominated deceleration gives critical insight into the functional meaning of attentional changes during different stages of threat proximity (Obrist, 1976; Davis and Lang, 2003; Löw et al., 2015): Anticipation of threat (decelerative responses to the CS) requires allocation of attentional resources, heightened vigilance, and facilitated sensory intake (“attentive freezing”). The goal of these attentional mechanisms is to mobilize and prepare the organism for later action responses (Lang and Bradley, 2010; Roelofs, 2017). In contrast, when the threat is most imminent (accelerative responses to the US), increased systemic activation and active defensive behavior are required, culminating in overt fight-or-flight responses (Davis and Lang, 2003; Lang and Bradley, 2013; Löw et al., 2015).

On the neural level, the US evoked a sharp fronto-central negative deflection from 50 to 200 ms, followed by a broader positive deflection from 200 to 350 ms which was maximal at rather centro-parietal electrode sites. These spatiotemporal characteristics match with previous studies investigating somatosensory ERPs to electrotactile stimuli (Miltner et al., 1989; Yamaguchi and Knight, 1991; Deguchi et al., 1996; Christmann et al., 2007; Kenntner-Mabiala et al., 2008; Wang et al., 2014; Nelson et al., 2015a; Wang and Tian, 2018). Both components seem to be sensitive to attentional modulations (Zaslansky et al., 1996; Eimer and Forster, 2003). The early negative complex is assumed to reflect mainly somatosensory processing of the aversive stimulus (Apkarian et al., 2005; Christmann et al., 2007). In contrast, the later positivity, which concurs with the typical P3 period (Yamaguchi and Knight, 1991), has been linked to rather top-down regulated affective and cognitive evaluation processing (Christmann et al., 2007; Kenntner-Mabiala et al., 2008; Valentini et al., 2013). In the present study, amplitudes during both periods were similar for the acquisition trainings of CS set 1, set 2, and set 3, providing evidence that repeated US presentations did not weaken somatosensory processing and attentional engagement with the aversive shock. In sum, peripheral physiology and ERP markers provide evidence that the US induced elevated arousal and increased recruitment of attentional resources during all three acquisition training phases. Importantly, unconditioned responses did not habituate over time.

Rapid learning about changing threat contingencies allows to predict harm in the future and can be critical for survival (LeDoux and Daw, 2018). A crucial goal of attention is to facilitate and accelerate the detection of potential danger (Mogg and Bradley, 1998; Wieser and Keil, 2020). Nevertheless, hypervigilance (Parsons and Ressler, 2013), biased attention toward threat (Burris et al., 2019), delayed attentional disengagement from threat (Amir et al., 2003), and overgeneralization of threat to harmless stimuli (Dunsmoor and Paz, 2015; Nelson et al., 2015b) are core symptoms of several disorders related to clinical fear. Specifically, patients with anxiety disorders display heightened and less flexible neural reactivity to threat (Moser et al., 2008; Mueller et al., 2009; MacNamara and Proudfit, 2014; Kujawa et al., 2015), which may

also be a meaningful predictor for treatment outcome (Stange et al., 2017). Furthermore, faster fear conditioning (Lissek et al., 2005) and delayed fear extinction (Duits et al., 2015) have been discussed as potential mediators in the etiology of anxiety disorders. Although there is evidence for attentional biases in clinical fear, some studies report contradictory findings (Holmes et al., 2008; Mueller et al., 2009; Weinberg and Hajcak, 2011; Weinberg et al., 2016). Moreover, the precise temporal dynamics of attentional threat biases and underlying mechanisms remain largely unknown (MacNamara et al., 2013). In the present study, we introduce sequential-set fear conditioning as a suitable tool to study the speed of neural threat learning. Thus, our novel paradigm may open new avenues to explore which processing stages contribute to aberrant threat processing in pathological fear. This knowledge might, in turn, lay the foundation to design more focused and tailored interventions to efficiently reduce pathological processing biases and to improve attentional control (Cisler and Koster, 2010; Wieser and Keil, 2020).

Although our data provide striking insights into the temporal unfolding of brain circuits during fear learning, there are some limitations. Strengthening the validity of our results, successful fear acquisition could even be probed within individual stimulus sets (e.g., $CS+_1$ versus $CS-_1$). For only the 33–60 ms period, averaging across all CS+/CS- sets was required to detect significantly enhanced CS+ amplitudes. This finding converges with our observation that short-latency effects only occurred during the last five conditioning trials, i.e., the signal-to-noise ratio is insufficient for a single CS set. It should also be kept in mind that there are more trials in the extinction training than in the acquisition training. This imbalance impedes the direct comparison between both experimental stages. Due to the limited spatial resolution of EEG, anatomical correlates of the reported neural processes remain vague, and future studies should combine sequential-set conditioning with simultaneous EEG-fMRI.

5. Conclusion

In conclusion, *sequential-set* fear conditioning provides a powerful design to unravel spatio-temporal dynamics of neural processes during learning about threats. By averaging across CS+/CS- sets, we guarantee a sufficiently high number of trials to detect changes in associative strength during learning and to study habituation-probe neural processes that are of particular relevance for the formation of emotional memories. While several studies have investigated electrocortical correlates of fear conditioning (Miskovic and Keil, 2012), the learning curve of neural processes has so far been neglected in human research. Our paradigm provides a valuable tool to further our understanding of the temporal unfolding of early (< 100 ms), mid-latency, and late neural processes. Developing a more detailed understanding about temporal characteristics of fear learning may have broad implications on neurobiological models of pathological fear and help to identify neurophysiological treatment targets in anxiety and related disorders.

Author contributions

M.F.J.S., A.W., M.M., B.S., and E.M.M. conceived and designed the study paradigm. M.F.J.S., A.W., and M.M. collected and preprocessed the data. M.F.J.S., A.W., M.M., and E.M.M. analyzed the data. M.F.J.S. and E.M.M. interpreted the data. M.F.J.S. and E.M.M. drafted the manuscript, and A.W., M.M., and B.S. provided critical revisions. M.F.J.S. created the figures. M.F.J.S. made the data, analysis scripts, code-books, and research materials publicly available. All of the authors discussed the results, commented on the article, and approved the final manuscript for submission.

Declaration of Competing Interest

The authors declare no competing financial interests.

Acknowledgments

M.F.J.S. was supported by the Research Training Group (RTG) 2271 “Breaking Expectations: Expectation Maintenance versus Change in the Context of Expectation Violations” (grant number DFG 290878970-GRK2271, project 6) at the University of Marburg, funded by the Deutsche Forschungsgemeinschaft (DFG; German Research Foundation). M.F.J.S. received a Poster Award for this project at the RTG 2271 Meeting in Hirschegg (Austria) in 2019. In addition, M.F.J.S. received a Research Travel Award from the Society for Psychophysiological Research (SPR) to present parts of this work in preliminary form at the 59th Annual Meeting in Washington, D.C. in 2019. M.F.J.S. was also supported by the DFG grant MU3535/2-3, awarded to E.M.M. A.W. was supported by the Marburg University Research Academy (MARA) and the German Federal Ministry of Education and Research (BMBF, grant/award number FKZ 01EE1402E). B.S. was supported by the DFG grant STR1146/15-1. Open access publishing was funded by the RTG 2271 at the University of Marburg and by the Open Access Publication Fund of the University of Giessen. All authors are members of the Center for Mind, Brain and Behavior (CMBB), a joint research center of the University of Marburg and the University of Giessen at the Research Campus Central Hessen. Address correspondence to Matthias F.J. Sperl, Department of Psychology, Personality Psychology and Assessment, University of Marburg, 35032 Marburg, Germany. Email: matthias.sperl@staff.uni-marburg.de

Supplementary materials

Supplementary material associated with this article can be found, in the online version, at doi:10.1016/j.neuroimage.2020.117569. Open Practices: De-identified data (for analyses described in this manuscript along with a code-book and the data analysis scripts) and research materials have been made publicly available via Zenodo and can be accessed at https://doi.org/10.5281/zenodo.4294603.

References

Adhikari, A., Lerner, T.N., Finkelstein, J., Pak, S., Jennings, J.H., Davidson, T.J., Ferenczi, E., Gunaydin, L.A., Mirzabekov, J.J., Ye, L., Kim, S.-Y., Lei, A., Deisseroth, K., 2015. Basomedial amygdala mediates top-down control of anxiety and fear. Nature 527, 179–185. https://doi.org/10.1038/nature15698.

Amaral, D.G., Behniea, H., Kelly, J.L., 2003. Topographic organization of projections from the amygdala to the visual cortex in the macaque monkey. Neuroscience 118, 1099–1120. https://doi.org/10.1016/S0306-4522(02)01001-1.

Amir, N., Elias, J., Klumpp, H., Przeworski, A., 2003. Attentional bias to threat in social phobia: facilitated processing of threat or difficulty disengaging attention from threat? Behav. Res. Ther. 41, 1325–1335. https://doi.org/10.1016/s0005-7967(03)00039-1.

Anderson, B., 2011. There is no such thing as attention. Front. Psychol. 2, 246. https://doi.org/10.3389/fpsyg.2011.00246.

Apkarian, A.V., Bushnell, M.C., Treede, R.-D., Zubieta, J.-K., 2005. Human brain mechanisms of pain perception and regulation in health and disease. Eur. J. Pain 9, 463–484. https://doi.org/10.1016/j.ejpain.2004.11.001.

Auerbach, R.P., Tarlow, N., Bondy, E., Stewart, J.G., Aguirre, B., Kaplan, C., Yang, W., Pizzagalli, D.A., 2016. Electrocortical reactivity during self-referential processing in female youth with borderline personality disorder. Biol. Psychiatry Cogn. Neurosci. Neuroimaging 1, 335–344. https://doi.org/10.1016/j.bpsc.2016.04.004.

Bacigalupo, F., Luck, S.J., 2018. Event-related potential components as measures of aversive conditioning in humans. Psychophysiology 55, 13015. https://doi.org/10.1111/psyp.13015.

Bailey, N.W., Freedman, G., Raj, K., Sullivan, C.M., Rogasch, N.C., Chung, S.W., Hoy, K.E., Chambers, R., Hassed, C., van Dam, N.T., Koenig, T., Fitzgerald, P.B., 2019. Mindfulness meditators show altered distributions of early and late neural activity markers of attention in a response inhibition task. PLoS One 14, 0203096. https://doi.org/10.1371/journal.pone.0203096.

Benedek, M., Kaernbach, C., 2010a. A continuous measure of phasic electrodermal activity. J. Neurosci. Methods 190, 80–91. https://doi.org/10.1016/j.jneumeth.2010.04.028.

Benedek, M., Kaernbach, C., 2010b. Decomposition of skin conductance data by means of nonnegative deconvolution. Psychophysiology 47, 647–658. https://doi.org/10.1111/j.1469-8986.2009.00972.x.

Blanchard, D.C., Griebel, G., Pobbe, R., Blanchard, R.J., 2011. Risk assessment as an evolved threat detection and analysis process. Neurosci. Biobehav. Rev. 35, 991–998. https://doi.org/10.1016/j.neubiorev.2010.10.016.

Blau, V.C., Maurer, U., Tottenham, N., McCandliss, B.D., 2007. The face-specific N170 component is modulated by emotional facial expression. Behav. Brain Funct. 3, 7. https://doi.org/10.1186/1744-9081-3-7.

Boucsein, W., Fowles, D.C., Grimnes, S., Ben-Shakhar, G., Roth, W.T., Dawson, M.E., Filion, D.L., 2012. Publication recommendations for electrodermal measurements. Psychophysiology 49, 1017–1034. https://doi.org/10.1111/j.1469-8986.2012.01384.x.
Bouton, M.E., 2017. Extinction: behavioral mechanisms and their implications. In: Menzel, R., Byrne, J.H. (Eds.), Learning and Memory, Volume 1: Learning Theory and Behavior. Academic Press, Oxford, pp. 61–83 https://doi.org/10.1016/B978-0-12-809324-5.21006-7.
Bradley, M.M., 2009. Natural selective attention: orienting and emotion. Psychophysiology 46, 1–11. https://doi.org/10.1111/j.1469-8986.2008.00702.x.
Bradley, M.M., Moulder, B., Lang, P.J., 2005. When good things go bad: the reflex physiology of defense. Psychol. Sci. 16, 468–473. https://doi.org/10.1111/j.0956-7976.2005.01558.x.
Braeutigam, S., Bailey, A.J., Swithenby, S.J., 2001. Task-dependent early latency (30-60 ms) visual processing of human faces and other objects. Neuroreport 12, 1531–1536. https://doi.org/10.1097/00001756-200105250-00046.
Bröckelmann, A.-K., Steinberg, C., Elling, L., Zwanzger, P., Pantev, C., Junghöfer, M., 2011. Emotion-associated tones attract enhanced attention at early auditory processing: magnetoencephalographic correlates. J. Neurosci. 31, 7801–7810. https://doi.org/10.1523/JNEUROSCI.6236-10.2011.
Bublatzky, F., Flaisch, T., Stockburger, J., Schmälzle, R., Schupp, H.T., 2010. The interaction of anticipatory anxiety and emotional picture processing: an event-related brain potential study. Psychophysiology 47, 687–696. https://doi.org/10.1111/j.1469-8986.2010.00966.x.
Bublatzky, F., Schupp, H.T., 2012. Pictures cueing threat: brain dynamics in viewing explicitly instructed danger cues. Soc. Cogn. Affect. Neurosci. 7, 611–622. https://doi.org/10.1093/scan/nsr032.
Büchel, C., Morris, J., Dolan, R.J., Friston, K.J., 1998. Brain systems mediating aversive conditioning: an event-related fMRI study. Neuron 20, 947–957. https://doi.org/10.1016/S0896-6273(00)80476-6.
Burris, J.L., Buss, K., LoBue, V., Pérez-Edgar, K., Field, A.P., 2019. Biased attention to threat and anxiety: on taking a developmental approach. J. Exp. Psychopathol. 10, 204380871986071. https://doi.org/10.1177/2043808719860717.
Caharel, S., d'Arripe, O., Ramon, M., Jacques, C., Rossion, B., 2009. Early adaptation to repeated unfamiliar faces across viewpoint changes in the right hemisphere: evidence from the N170 ERP component. Neuropsychologia 47, 639–643. https://doi.org/10.1016/j.neuropsychologia.2008.11.016.
Calhoon, G.G., Tye, K.M., 2015. Resolving the neural circuits of anxiety. Nat. Neurosci. 18, 1394–1404. https://doi.org/10.1038/nn.4101.
Camfield, D.A., Mills, J., Kornfeld, E.J., Croft, R.J., 2016. Modulation of the N170 with classical conditioning: the use of emotional imagery and acoustic startle in healthy and depressed participants. Front. Hum. Neurosci. 10, 337. https://doi.org/10.3389/fnhum.2016.00337.
Castegnetti, G., Tzovara, A., Staib, M., Paulus, P.C., Hofer, N., Bach, D.R., 2016. Modeling fear-conditioned bradycardia in humans. Psychophysiology 53, 930–939. https://doi.org/10.1111/psyp.12637.
Chen, Y., Zhu, B., Shou, T., 2009. Anatomical evidence for the projections from the basal nucleus of the amygdala to the primary visual cortex in the cat. Neurosci. Lett. 453, 126–130. https://doi.org/10.1016/j.neulet.2009.02.022.
Christmann, C., Koeppe, C., Braus, D.F., Ruf, M., Flor, H., 2007. A simultaneous EEG-fMRI study of painful electric stimulation. NeuroImage 34, 1428–1437. https://doi.org/10.1016/j.neuroimage.2006.11.006.
Cisler, J.M., Koster, E.H.W., 2010. Mechanisms of attentional biases towards threat in anxiety disorders: an integrative review. Clin. Psychol. Rev. 30, 203–216. https://doi.org/10.1016/j.cpr.2009.11.003.
Clark, V.P., Fan, S., Hillyard, S.A., 1994. Identification of early visual evoked potential generators by retinotopic and topographic analyses. Hum. Brain Mapp. 2, 170–187. https://doi.org/10.1002/hbm.460020306.
Clark, V.P., Hillyard, S.A., 1996. Spatial selective attention affects early extrastriate but not striate components of the visual evoked potential. J. Cogn. Neurosci. 8, 387–402. https://doi.org/10.1162/jocn.1996.8.5.387.
Clayson, P.E., Carbine, K.A., Baldwin, S.A., Larson, M.J., 2019. Methodological reporting behavior, sample sizes, and statistical power in studies of event-related potentials: barriers to reproducibility and replicability. Psychophysiology 56, 13437. https://doi.org/10.1111/psyp.13437.
Codispoti, M., Ferrari, V., Bradley, M.M., 2006. Repetitive picture processing: autonomic and cortical correlates. Brain Res. 1068, 213–220. https://doi.org/10.1016/j.brainres.2005.11.009.
Codispoti, M., Ferrari, V., Bradley, M.M., 2007. Repetition and event-related potentials: distinguishing early and late processes in affective picture perception. J. Cogn. Neurosci. 19, 577–586. https://doi.org/10.1162/jocn.2007.19.4.577.
Cohen, J., 1988. Statistical Power Analysis for the Behavioral Sciences. Lawrence Erlbaum Associates, Hillsdale, NJ https://doi.org/10.4324/9780203771587.
Cohen, J., 1992. A power primer. Psychol. Bull. 112, 155–159. https://doi.org/10.1037//0033-2909.112.1.155.
Cohen, M.X., 2014. Analyzing Neural Time Series Data: Theory and Practice. MIT Press, Cambridge, MA https://doi.org/10.7551/mitpress/9609.001.0001.
Craske, M.G., Hermans, D., Vervliet, B., 2018. State-of-the-art and future directions for extinction as a translational model for fear and anxiety. Philos. Trans. R. Soc. Lond. B Biol. Sci. 373, 20170025. https://doi.org/10.1098/rstb.2017.0025.
Cuthbert, B.N., Schupp, H.T., Bradley, M.M., Birbaumer, N., Lang, P.J., 2000. Brain potentials in affective picture processing: covariation with autonomic arousal and affective report. Biol. Psychol. 52, 95–111. https://doi.org/10.1016/S0301-0511(99)00044-7.
Davis, M., Lang, P.J., 2003. Emotion. In: Gallagher, M., Nelson, R.J., Weiner, I.B. (Eds.), Handbook of Psychology: Volume 3, Biological Psychology. Wiley, Hoboken, NJ, pp. 405–439 https://doi.org/10.1002/0471264385.wei0315.
Davis, M., Whalen, P.J., 2001. The amygdala: vigilance and emotion. Mol. Psychiatry 6, 13–34. https://doi.org/10.1038/sj.mp.4000812.
Deane, G.E., Zeaman, D., 1958. Human heart rate during anxiety. Percept. Mot. Skills 8, 103–106. https://doi.org/10.2466/pms.1958.8.3.103.
Deguchi, K., Takeuchi, H., Touge, T., Kamoda, M., Tsukaguchi, M., Sasaki, I., Nishioka, M., 1996. Significance of cognitive function in the elicitation of sympathetic skin response in healthy humans. J. Auton. Nerv. Syst. 61, 123–127. https://doi.org/10.1016/S0165-1838(96)00067-7.
Desjardins, J.A., Segalowitz, S.J., 2013. Deconstructing the early visual electrocortical responses to face and house stimuli. J. Vis. 13, 22. https://doi.org/10.1167/13.5.22.
Dimigen, O., 2020. Optimizing the ICA-based removal of ocular EEG artifacts from free viewing experiments. NeuroImage 207, 116117. https://doi.org/10.1016/j.neuroimage.2019.116117.
Duits, P., Cath, D.C., Lissek, S., Hox, J.J., Hamm, A.O., Engelhard, I.M., van den Hout, M.A., Baas, J.M.P., 2015. Updated meta-analysis of classical fear conditioning in the anxiety disorders. Depress. Anxiety 32, 239–253. https://doi.org/10.1002/da.22353.
Duits, P., Richter, J., Baas, J.M.P., Engelhard, I.M., Limberg-Thiesen, A., Heitland, I., Hamm, A.O., Cath, D.C., 2017. Enhancing effects of contingency instructions on fear acquisition and extinction in anxiety disorders. J. Abnorm. Psychol. 126, 378–391. https://doi.org/10.1037/abn0000266.
Dunsmoor, J.E., Paz, R., 2015. Fear generalization and anxiety: behavioral and neural mechanisms. Biol. Psychiatry 78, 336–343. https://doi.org/10.1016/j.biopsych.2015.04.010.
Ebrahimi, C., Gechter, J., Lueken, U., Schlagenhauf, F., Wittchen, H.-U., Hamm, A.O., Ströhle, A., 2020. Augmenting extinction learning with D-cycloserine reduces return of fear: a randomized, placebo-controlled fMRI study. Neuropsychopharmacology 45, 499–506. https://doi.org/10.1038/s41386-019-0552-z.
Eimer, M., 2000. Attentional modulations of event-related brain potentials sensitive to faces. Cogn. Neuropsychol. 17, 103–116. https://doi.org/10.1080/026432900380517.
Eimer, M., 2011. The face-sensitive N170 component of the event-related brain potential. In: Calder, A.J., Rhodes, G., Johnson, M.H., Haxby, J.V. (Eds.), The Oxford Handbook of Face Perception. Oxford University Press, New York, NY, pp. 329–344 https://doi.org/10.1093/oxfordhb/9780199559053.013.0017.
Eimer, M., 2018. The time course of spatial attention: insights from event-related brain potentials. In: Nobre, A.C., Kastner, S. (Eds.), The Oxford Handbook of Attention. Oxford University Press, New York, NY, pp. 289–317. https://doi.org/10.1093/oxfordhb/9780199675111.013.006.
Eimer, M., Forster, B., 2003. Modulations of early somatosensory ERP components by transient and sustained spatial attention. Exp. Brain Res. 151, 24–31. https://doi.org/10.1007/s00221-003-1437-1.
Eimer, M., Holmes, A., McGlone, F.P., 2003. The role of spatial attention in the processing of facial expression: an ERP study of rapid brain responses to six basic emotions. Cogn. Affect. Behav. Neurosci. 3, 97–110. https://doi.org/10.3758/cabn.3.2.97.
Erickson, M.A., Kappenman, E.S., Luck, S.J., 2018. High temporal resolution measurement of cognitive and affective processes in psychopathology: what electroencephalography and magnetoencephalography can tell us about mental illness. Biol. Psychiatry Cogn. Neurosci. Neuroimaging 3, 4–6. https://doi.org/10.1016/j.bpsc.2017.11.008.
Fadok, J.P., Krabbe, S., Markovic, M., Courtin, J., Xu, C., Massi, L., Botta, P., Bylund, K., Müller, C., Kovacevic, A., Tovote, P., Lüthi, A., 2017. A competitive inhibitory circuit for selection of active and passive fear responses. Nature 542, 96–100. https://doi.org/10.1038/nature21047.
Faul, F., Erdfelder, E., Lang, A.-G., Buchner, A., 2007. G*Power 3: a flexible statistical power analysis program for the social, behavioral, and biomedical sciences. Behav. Res. Methods 39, 175–191. https://doi.org/10.3758/BF03193146.
Feng, P., Zheng, Y., Feng, T., 2015. Spontaneous brain activity following fear reminder of fear conditioning by using resting-state functional MRI. Sci. Rep. 5, 16701. https://doi.org/10.1038/srep16701.
Ferreira de Sá, D.S., Michael, T., Wilhelm, F.H., Peyk, P., 2019. Learning to see the threat: temporal dynamics of ERPs of motivated attention in fear conditioning. Soc. Cogn. Affect. Neurosci. 14, 189–203. https://doi.org/10.1093/scan/nsy103.
Flores, Á., Fullana, M.À., Soriano-Mas, C., Andero, R., 2018. Lost in translation: how to upgrade fear memory research. Mol. Psychiatry 23, 2122–2132. https://doi.org/10.1038/s41380-017-0006-0.
Freese, J.L., Amaral, D.G., 2005. The organization of projections from the amygdala to visual cortical areas TE and V1 in the macaque monkey. J. Comp. Neurol. 486, 295–317. https://doi.org/10.1002/cne.20520.
Fullana, M.A., Harrison, B.J., Soriano-Mas, C., Vervliet, B., Cardoner, N., Avila-Parcet, A., Radua, J., 2016. Neural signatures of human fear conditioning: an updated and extended meta-analysis of fMRI studies. Mol. Psychiatry 21, 500–508. https://doi.org/10.1038/mp.2015.88.
Gao, C., Conte, S., Richards, J.E., Xie, W., Hanayik, T., 2019. The neural sources of N170: understanding timing of activation in face-selective areas. Psychophysiology 56, 13336. https://doi.org/10.1111/psyp.13336.
Gelder, B.de, Meeren, H.K.M., Righart, R., van den Stock, J., van de Riet, W.A.C., Tamietto, M., 2006. Beyond the face: exploring rapid influences of context on face processing. Prog. Brain Res. 155, 37–48. https://doi.org/10.1016/S0079-6123(06)55003-4.
Gianotti, L.R.R., Faber, P.L., Schuler, M., Pascual-Marqui, R.D., Kochi, K., Lehmann, D., 2008. First valence, then arousal: the temporal dynamics of brain electric activity evoked by emotional stimuli. Brain Topogr. 20, 143–156. https://doi.org/10.1007/s10548-007-0041-2.
Ginsberg, S., Thysell, R.V., 1966. Heart rate response as a function of shock intensity. Psychon. Sci. 6, 475–476. https://doi.org/10.3758/BF03328098.
Golkar, A., Bellander, M., Öhman, A., 2013. Temporal properties of fear extinction – does time matter? Behav. Neurosci. 127, 59–69. https://doi.org/10.1037/a0030892.

Gomez Gonzalez, C.M., Clark, V.P., Fan, S., Luck, S.J., Hillyard, S.A., 1994. Sources of attention-sensitive visual event-related potentials. Brain Topogr. 7, 41–51. https://doi.org/10.1007/BF01184836.

Greco, J.A., Liberzon, I., 2016. Neuroimaging of fear-associated learning. Neuropsychopharmacology 41, 320–334. https://doi.org/10.1038/npp.2015.255.

Greenhouse, S.W., Geisser, S., 1959. On methods in the analysis of profile data. Psychometrika 24, 95–112. https://doi.org/10.1007/BF02289823.

Gupta, R.S., Kujawa, A., Vago, D.R., 2019. The neural chronometry of threat-related attentional bias: event-related potential (ERP) evidence for early and late stages of selective attentional processing. Int. J. Psychophysiol. 146, 20–42. https://doi.org/10.1016/j.ijpsycho.2019.08.006.

Haaker, J., Maren, S., Andreatta, M., Merz, C.J., Richter, J., Richter, S.H., Meir Drexler, S., Lange, M.D., Jüngling, K., Nees, F., Seidenbecher, T., Fullana, M.A., Wotjak, C.T., Lonsdorf, T.B., 2019. Making translation work: harmonizing cross-species methodology in the behavioural neuroscience of Pavlovian fear conditioning. Neurosci. Biobehav. Rev. 107, 329–345. https://doi.org/10.1016/j.neubiorev.2019.09.020.

Habermann, M., Weusmann, D., Stein, M., Koenig, T., 2018. A student's guide to randomization statistics for multichannel event-related potentials using Ragu. Front. Neurosci. 12, 355. https://doi.org/10.3389/fnins.2018.00355.

Hajcak, G., Dunning, J.P., Foti, D., 2009. Motivated and controlled attention to emotion: time-course of the late positive potential. Clin. Neurophysiol. 120, 505–510. https://doi.org/10.1016/j.clinph.2008.11.028.

Hajcak, G., Foti, D., 2020. Significance? … Significance! Empirical, methodological, and theoretical connections between the late positive potential and P300 as neural responses to stimulus significance: an integrative review. Psychophysiology 57, 13570. https://doi.org/10.1111/psyp.13570.

Hajcak, G., Jackson, F., Ferri, J., Weinberg, A., 2018. Emotion and attention. In: Barrett, L.F., Lewis, M., Haviland-Jones, J.M. (Eds.), Handbook of Emotions. Guilford Press, New York, NY, pp. 595–609.

Hajcak, G., Klawohn, J., Meyer, A., 2019. The utility of event-related potentials in clinical psychology. Annu. Rev. Clin. Psychol. 15, 71–95. https://doi.org/10.1146/annurev-clinpsy-050718-095457.

Hajcak, G., MacNamara, A., Olvet, D.M., 2010. Event-related potentials, emotion, and emotion regulation: an integrative review. Dev. Neuropsychol. 35, 129–155. https://doi.org/10.1080/87565640903526504.

Hartley, N.D., Gaulden, A.D., Báldi, R., Winters, N.D., Salimando, G.J., Rosas-Vidal, L.E., Jameson, A., Winder, D.G., Patel, S., 2019. Dynamic remodeling of a basolateral-to-central amygdala glutamatergic circuit across fear states. Nat. Neurosci. 22, 2000–2012. https://doi.org/10.1038/s41593-019-0528-7.

Heinig, I., Pittig, A., Richter, J., Hummel, K., Alt, I., Dickhöver, K., Gamer, J., Hollandt, M., Koelkebeck, K., Maenz, A., Tennie, S., Totzeck, C., Yang, Y., Arolt, V., Deckert, J., Domschke, K., Fydrich, T., Hamm, A., Hoyer, J., Kircher, T., Lueken, U., Margraf, J., Neudeck, P., Pauli, P., Rief, W., Schneider, S., Straube, B., Ströhle, A., Wittchen, H.-U., 2017. Optimizing exposure-based CBT for anxiety disorders via enhanced extinction: design and methods of a multicentre randomized clinical trial. Int. J. Methods Psychiatr. Res. 26, e1560. https://doi.org/10.1002/mpr.1560.

Hintze, P., Junghöfer, M., Bruchmann, M., 2014. Evidence for rapid prefrontal emotional evaluation from visual evoked responses to conditioned gratings. Biol. Psychol. 99, 125–136. https://doi.org/10.1016/j.biopsycho.2014.03.010.

Hollandt, M., Wroblewski, A., Yang, Y., Ridderbusch, I.C., Kircher, T., Hamm, A.O., Straube, B., Richter, J., 2020. Facilitating translational science in anxiety disorders by adjusting extinction training in the laboratory to exposure-based therapy procedures. Transl. Psychiatry 10, 110. https://doi.org/10.1038/s41398-020-0786-x.

Holmes, A., Nielsen, M.K., Green, S., 2008. Effects of anxiety on the processing of fearful and happy faces: an event-related potential study. Biol. Psychol. 77, 159–173. https://doi.org/10.1016/j.biopsycho.2007.10.003.

Holmes, A., Winston, J.S., Eimer, M., 2005. The role of spatial frequency information for ERP components sensitive to faces and emotional facial expression. Brain Res. Cogn. Brain Res. 25, 508–520. https://doi.org/10.1016/j.cogbrainres.2005.08.003.

Huffmeijer, R., Bakermans-Kranenburg, M.J., Alink, L.R.A., van Ijzendoorn, M.H., 2014. Reliability of event-related potentials: the influence of number of trials and electrodes. Physiol. Behav. 130, 13–22. https://doi.org/10.1016/j.physbeh.2014.03.008.

Janak, P.H., Tye, K.M., 2015. From circuits to behaviour in the amygdala. Nature 517, 284–292. https://doi.org/10.1038/nature14188.

Jayachandran, M., Linley, S.B., Schlecht, M., Mahler, S.V., Vertes, R.P., Allen, T.A., 2019. Prefrontal pathways provide top-down control of memory for sequences of events. Cell Rep. 28, 640–654. e6 https://doi.org/10.1016/j.celrep.2019.06.053 .

Jeffreys, D.A., Axford, J.G., 1972. Source locations of pattern-specific components of human visual evoked potentials. I. Component of striate cortical origin. Exp. Brain Res. 16, 1–21. https://doi.org/10.1007/bf00233371.

Keil, A., Debener, S., Gratton, G., Junghöfer, M., Kappenman, E.S., Luck, S.J., Luu, P., Miller, G.A., Yee, C.M., 2014. Committee report: publication guidelines and recommendations for studies using electroencephalography and magnetoencephalography. Psychophysiology 51, 1–21. https://doi.org/10.1111/psyp.12147.

Keil, A., Stolarova, M., Moratti, S., Ray, W.J., 2007. Adaptation in human visual cortex as a mechanism for rapid discrimination of aversive stimuli. NeuroImage 36, 472–479. https://doi.org/10.1016/j.neuroimage.2007.02.048.

Kenntner-Mabiala, R., Andreatta, M., Wieser, M.J., Mühlberger, A., Pauli, P., 2008. Distinct effects of attention and affect on pain perception and somatosensory evoked potentials. Biol. Psychol. 78, 114–122. https://doi.org/10.1016/j.biopsycho.2008.01.007.

Kirchner, H., Barbeau, E.J., Thorpe, S.J., Régis, J., Liégeois-Chauvel, C., 2009. Ultra-rapid sensory responses in the human frontal eye field region. J. Neurosci. 29, 7599–7606. https://doi.org/10.1523/JNEUROSCI.1233-09.2009.

Kluge, C., Bauer, M., Leff, A.P., Heinze, H.-J., Dolan, R.J., Driver, J., 2011. Plasticity of human auditory-evoked fields induced by shock conditioning and contingency reversal. Proc. Natl. Acad. Sci. USA 108, 12545–12550. https://doi.org/10.1073/pnas.1016124108.

Klumpers, F., Raemaekers, M.A.H.L., Ruigrok, A.N.V., Hermans, E.J., Kenemans, J.L., Baas, J.M.P., 2010. Prefrontal mechanisms of fear reduction after threat offset. Biol. Psychiatry 68, 1031–1038. https://doi.org/10.1016/j.biopsych.2010.09.006.

Klumpp, H., Shankman, S.A., 2018. Using event-related potentials and startle to evaluate time course in anxiety and depression. Biol. Psychiatry Cogn. Neurosci. Neuroimaging 3, 10–18. https://doi.org/10.1016/j.bpsc.2017.09.004.

Koenig, T., Kottlow, M., Stein, M., Melie-García, L., 2011. Ragu: a free tool for the analysis of EEG and MEG event-related scalp field data using global randomization statistics. Comput. Intell. Neurosci. 2011, 938925. https://doi.org/10.1155/2011/938925.

Koenig, T., Melie-García, L., 2009. Statistical analysis of multichannel scalp field data. In: Michel, C.M., Koenig, T., Brandeis, D., Gianotti, L.R.R., Wackermann, J. (Eds.), Electrical Neuroimaging. Cambridge University Press, Cambridge, pp. 169–190 https://doi.org/10.1017/CBO9780511596889.009.

Kret, M.E., Gelder, B.de, 2012. A review on sex differences in processing emotional signals. Neuropsychologia 50, 1211–1221. https://doi.org/10.1016/j.neuropsychologia.2011.12.022.

Kujawa, A., MacNamara, A., Fitzgerald, K.D., Monk, C.S., Phan, K.L., 2015. Enhanced neural reactivity to threatening faces in anxious youth: evidence from event-related potentials. J. Abnorm. Child Psychol. 43, 1493–1501. https://doi.org/10.1007/s10802-015-0029-4.

Kumar, T., Jha, S.K., Kline, A.E., 2012. Sleep deprivation impairs consolidation of cued fear memory in rats. PLoS One 7, 47042. https://doi.org/10.1371/journal.pone.0047042.

LaBar, K.S., Gatenby, J.C., Gore, J.C., LeDoux, J.E., Phelps, E.A., 1998. Human amygdala activation during conditioned fear acquisition and extinction: a mixed-trial fMRI study. Neuron 20, 937–945 https://doi.org/10.1016/S0896-6273(00)80475-4.

Lamme, V.A.F., Roelfsema, P.R., 2000. The distinct modes of vision offered by feedforward and recurrent processing. Trends Neurosci. 23, 571–579. https://doi.org/10.1016/s0166-2236(00)01657-x.

Lang, P.J., Bradley, M.M., 2010. Emotion and the motivational brain. Biol. Psychol. 84, 437–450. https://doi.org/10.1016/j.biopsycho.2009.10.007.

Lang, P.J., Bradley, M.M., 2013. Appetitive and defensive motivation: goal-directed or goal-determined? Emot. Rev. 5, 230–234. https://doi.org/10.1177/1754073913477511.

Lang, P.J., Bradley, M.M., Cuthbert, B.N., 1997. Motivated attention: affect, activation, and action. In: Lang, P.J., Simons, R.F., Balaban, M.T. (Eds.), Attention and Orienting: Sensory and Motivational Processes. Erlbaum, Hillsdale, NJ, pp. 97–135 https://doi.org/10.4324/9780203726457.

Lavric, A., Pizzagalli, D.A., Forstmeier, S., 2004. When 'go' and 'nogo' are equally frequent: ERP components and cortical tomography. Eur. J. Neurosci. 20, 2483–2488. https://doi.org/10.1111/j.1460-9568.2004.03683.x.

LeDoux, J.E., 1995. Emotion: clues from the brain. Annu. Rev. Psychol. 46, 209–235. https://doi.org/10.1146/annurev.ps.46.020195.001233.

LeDoux, J.E., 2000. Emotion circuits in the brain. Annu. Rev. Neurosci. 23, 155–184. https://doi.org/10.1146/annurev.neuro.23.1.155.

LeDoux, J.E., 2014. Coming to terms with fear. Proc. Natl. Acad. Sci. USA 111, 2871–2878. https://doi.org/10.1073/pnas.1400335111.

LeDoux, J.E., Daw, N.D., 2018. Surviving threats: neural circuit and computational implications of a new taxonomy of defensive behaviour. Nat. Rev. Neurosci. 19, 269–282. https://doi.org/10.1038/nrn.2018.22.

Lehmann, D., Skrandies, W., 1980. Reference-free identification of components of checkerboard-evoked multichannel potential fields. Electroencephalogr. Clin. Neurophysiol. 48, 609–621. https://doi.org/10.1016/0013-4694(80)90419-8.

Lehmann, D., Skrandies, W., 1984. Spatial analysis of evoked potentials in man – a review. Prog. Neurobiol. 23, 227–250. https://doi.org/10.1016/0301-0082(84)90003-0.

Levita, L., Howsley, P., Jordan, J., Johnston, P., 2015. Potentiation of the early visual response to learned danger signals in adults and adolescents. Soc. Cogn. Affect. Neurosci. 10, 269–277. https://doi.org/10.1093/scan/nsu048.

Linkenkaer-Hansen, K., Palva, J.M., Sams, M., Hietanen, J.K., Aronen, H.J., Ilmoniemi, R.J., 1998. Face-selective processing in human extrastriate cortex around 120 ms after stimulus onset revealed by magneto- and electroencephalography. Neurosci. Lett. 253, 147–150. https://doi.org/10.1016/S0304-3940(98)00586-2.

Lipp, O.V., 2006. Human fear learning: contemporary procedures and measurement. In: Craske, M.G., Hermans, D., Vansteenwegen, D. (Eds.), Fear and Learning: From Basic Processes to Clinical Implications. American Psychological Association, Washington, D.C., pp. 37–52 https://doi.org/10.1037/11474-002.

Lipp, O.V., Vaitl, D., 1990. Reaction time task as unconditional stimulus. Comparing aversive and nonaversive unconditional stimuli. Pavlov. J. Biol. Sci. 25, 77–83. https://doi.org/10.1007/BF02964606.

Lissek, S., Powers, A.S., McClure, E.B., Phelps, E.A., Woldehawariat, G., Grillon, C., Pine, D.S., 2005. Classical fear conditioning in the anxiety disorders: a meta-analysis. Behav. Res. Ther. 43, 1391–1424. https://doi.org/10.1016/j.brat.2004.10.007.

Liu, Y., Huang, H., McGinnis-Deweese, M., Keil, A., Ding, M., 2012a. Neural substrate of the late positive potential in emotional processing. J. Neurosci. 32, 14563–14572. https://doi.org/10.1523/JNEUROSCI.3109-12.2012.

Liu, Y., Keil, A., Ding, M., 2012b. Effects of emotional conditioning on early visual processing: temporal dynamics revealed by ERP single-trial analysis. Hum. Brain Mapp. 33, 909–919. https://doi.org/10.1002/hbm.21259.

Logothetis, N.K., Pauls, J., Augath, M., Trinath, T., Oeltermann, A., 2001. Neurophysiological investigation of the basis of the fMRI signal. Nature 412, 150–157. https://doi.org/10.1038/35084005.

Lonsdorf, T.B., Menz, M.M., Andreatta, M., Fullana, M.A., Golkar, A., Haaker, J., Heitland, I., Hermann, A., Kuhn, M., Kruse, O., Meir Drexler, S., Meulders, A., Nees, F., Pittig, A., Richter, J., Römer, S., Shiban, Y., Schmitz, A., Straube, B., Vervliet, B.,

Wendt, J., Baas, J.M.P., Merz, C.J., 2017. Don't fear 'fear conditioning': methodological considerations for the design and analysis of studies on human fear acquisition, extinction, and return of fear. Neurosci. Biobehav. Rev. 77, 247–285. https://doi.org/10.1016/j.neubiorev.2017.02.026.

Löw, A., Weymar, M., Hamm, A.O., 2015. When threat is near, get out of here: dynamics of defensive behavior during freezing and active avoidance. Psychol. Sci. 26, 1706–1716. https://doi.org/10.1177/0956797615597332.

Luck, S.J., 2014. An Introduction to the Event-Related Potential Technique. MIT Press, Cambridge, MA.

Luck, S.J., Gaspelin, N., 2017. How to get statistically significant effects in any ERP experiment (and why you shouldn't). Psychophysiology 54, 146–157. https://doi.org/10.1111/psyp.12639.

Luck, S.J., Kappenman, E.S., 2019. Electroencephalography and event-related brain potentials. In: Cacioppo, J.T., Tassinary, L.G., Berntson, G.G. (Eds.), Handbook of Psychophysiology. Cambridge University Press, Cambridge, pp. 74–100 https://doi.org/10.1017/9781107415782.005.

MacNamara, A., Kappenman, E.S., Black, S.R., Bress, J.N., Hajcak, G., 2013. Integrating behavioral and electrocortical measures of attentional bias toward threat. In: Barrett, K.C., Fox, N.A., Morgan, G.A., Fidler, D.J., Daunhauer, L.A. (Eds.), Handbook of Self-Regulatory Processes in Development: New Directions and International Perspectives. Psychology Press, New York, NY, pp. 215–242 https://doi.org/10.4324/9780203080719.ch11.

MacNamara, A., Proudfit, G.H., 2014. Cognitive load and emotional processing in generalized anxiety disorder: electrocortical evidence for increased distractibility. J. Abnorm. Psychol. 123, 557–565. https://doi.org/10.1037/a0036997.

Manly, B.F.J., 2007. Randomization, Bootstrap and Monte Carlo Methods in Biology. Chapman & Hall/CRC, Boca Raton, Florida https://doi.org/10.1201/9781315273075.

Marek, R., Sun, Y., Sah, P., 2019. Neural circuits for a top-down control of fear and extinction. Psychopharmacology 236, 313–320. https://doi.org/10.1007/s00213-018-5033-2.

Maren, S., 2014. Nature and causes of the immediate extinction deficit: a brief review. Neurobiol. Learn. Mem. 113, 19–24. https://doi.org/10.1016/j.nlm.2013.10.012.

Margraf, J., 1994. MINI-DIPS: Diagnostisches Kurz-Interview bei psychischen Störungen (Diagnostic Interview for Mental Disorders – Short Version). Springer, Berlin.

Marin, M.-F., Barbey, F., Rosenbaum, B.L., Hammoud, M.Z., Orr, S.P., Milad, M.R., 2020. Absence of conditioned responding in humans: a bad measure or individual differences? Psychophysiology 57, 13350. https://doi.org/10.1111/psyp.13350.

Martinovic, J., Jones, A., Christiansen, P., Rose, A.K., Hogarth, L., Field, M., 2014. Electrophysiological responses to alcohol cues are not associated with Pavlovian-to-instrumental transfer in social drinkers. PLoS One 9, 94605. https://doi.org/10.1371/journal.pone.0094605.

Maurer, U., Brandeis, D., McCandliss, B.D., 2005. Fast, visual specialization for reading in English revealed by the topography of the N170 ERP response. Behav. Brain Funct. 1, 13. https://doi.org/10.1186/1744-9081-1-13.

McCullough, K.M., Morrison, F.G., Ressler, K.J., 2016. Bridging the gap: towards a cell-type specific understanding of neural circuits underlying fear behaviors. Neurobiol. Learn. Mem. 135, 27–39. https://doi.org/10.1016/j.nlm.2016.07.025.

McKone, E., Robbins, R., 2011. Are faces special? In: Calder, A.J., Rhodes, G., Johnson, M.H., Haxby, J.V. (Eds.) The Oxford Handbook of Face Perception. Oxford University Press, New York, NY, pp. 149–176 https://doi.org/10.1093/oxfordhb/9780199559053.013.0009.

McTeague, L.M., Gruss, L.F., Keil, A., 2015. Aversive learning shapes neuronal orientation tuning in human visual cortex. Nat. Commun. 6, 7823. https://doi.org/10.1038/ncomms8823.

Menz, M.M., Rihm, J.S., Büchel, C., 2016. REM sleep is causal to successful consolidation of dangerous and safety stimuli and reduces return of fear after extinction. J. Neurosci. 36, 2148–2160. https://doi.org/10.1523/JNEUROSCI.3083-15.2016.

Mertens, G., Boddez, Y., Sevenster, D., Engelhard, I.M., De Houwer, J., 2018. A review on the effects of verbal instructions in human fear conditioning: empirical findings, theoretical considerations, and future directions. Biol. Psychol. 137, 49–64. https://doi.org/10.1016/j.biopsycho.2018.07.002.

Michel, C.M., Murray, M.M., 2012. Towards the utilization of EEG as a brain imaging tool. NeuroImage 61, 371–385. https://doi.org/10.1016/j.neuroimage.2011.12.039.

Milad, M.R., Quirk, G.J., 2012. Fear extinction as a model for translational neuroscience: ten years of progress. Annu. Rev. Psychol. 63, 129–151. https://doi.org/10.1146/annurev.psych.121208.131631.

Miltner, W., Johnson, R., Braun, C., Larbig, W., 1989. Somatosensory event-related potentials to painful and non-painful stimuli: effects of attention. Pain 38, 303–312. https://doi.org/10.1016/0304-3959(89)90217-0.

Miskovic, V., Keil, A., 2012. Acquired fears reflected in cortical sensory processing: a review of electrophysiological studies of human classical conditioning. Psychophysiology 49, 1230–1241. https://doi.org/10.1111/j.1469-8986.2012.01398.x.

Mobbs, D., Hagan, C.C., Dalgleish, T., Silston, B., Prévost, C., 2015. The ecology of human fear: survival optimization and the nervous system. Front. Neurosci. 9, 55. https://doi.org/10.3389/fnins.2015.00055.

Mogg, K., Bradley, B.P., 1998. A cognitive-motivational analysis of anxiety. Behav. Res. Ther. 36, 809–848. https://doi.org/10.1016/s0005-7967(98)00063-1.

Mohanty, A., Sussman, T.J., 2013. Top-down modulation of attention by emotion. Front. Hum. Neurosci. 7, 102. https://doi.org/10.3389/fnhum.2013.00102.

Monfils, M.H., Holmes, E.A., 2018. Memory boundaries: opening a window inspired by reconsolidation to treat anxiety, trauma-related, and addiction disorders. Lancet Psychiatry 5, 1032–1042. https://doi.org/10.1016/S2215-0366(18)30270-0.

Moratti, S., Keil, A., Miller, G.A., 2006. Fear but not awareness predicts enhanced sensory processing in fear conditioning. Psychophysiology 43, 216–226. https://doi.org/10.1111/j.1464-8986.2006.00386.x.

Morel, S., Beaucousin, V., Perrin, M., George, N., 2012. Very early modulation of brain responses to neutral faces by a single prior association with an emotional context: evidence from MEG. NeuroImage 61, 1461–1470. https://doi.org/10.1016/j.neuroimage.2012.04.016.

Morel, S., Ponz, A., Mercier, M., Vuilleumier, P., George, N., 2009. EEG-MEG evidence for early differential repetition effects for fearful, happy and neutral faces. Brain Res. 1254, 84–98. https://doi.org/10.1016/j.brainres.2008.11.079.

Moser, J.S., Huppert, J.D., Duval, E., Simons, R.F., 2008. Face processing biases in social anxiety: an electrophysiological study. Biol. Psychol. 78, 93–103. https://doi.org/10.1016/j.biopsycho.2008.01.005.

Mueller, E.M., Hofmann, S.G., Santesso, D.L., Meuret, A.E., Bitran, S., Pizzagalli, D.A., 2009. Electrophysiological evidence of attentional biases in social anxiety disorder. Psychol. Med. 39, 1141. https://doi.org/10.1017/S0033291708004820.

Mueller, E.M., Pizzagalli, D.A., 2016. One-year-old fear memories rapidly activate human fusiform gyrus. Soc. Cogn. Affect. Neurosci. 11, 308–316. https://doi.org/10.1093/scan/nsv122.

Mueller, E.M., Sperl, M.F.J., Panitz, C., 2019. Aversive imagery causes de novo fear conditioning. Psychol. Sci. 30, 1001–1015. https://doi.org/10.1177/0956797619842261.

Mueller, E.M., Stemmler, G., Hennig, J., Wacker, J., 2013. 5-HTTLPR and anxiety modulate brain-heart covariation. Psychophysiology 50, 441–453. https://doi.org/10.1111/psyp.12016.

Muench, H.M., Westermann, S., Pizzagalli, D.A., Hofmann, S.G., Mueller, E.M., 2016. Self-relevant threat contexts enhance early processing of fear-conditioned faces. Biol. Psychol. 121, 194–202. https://doi.org/10.1016/j.biopsycho.2016.07.017.

Murray, M.M., Brunet, D., Michel, C.M., 2008. Topographic ERP analyses: a step-by-step tutorial review. Brain Topogr. 20, 249–264. https://doi.org/10.1007/s10548-008-0054-5.

Myers, K.M., Davis, M., 2007. Mechanisms of fear extinction. Mol. Psychiatry 12, 120–150. https://doi.org/10.1038/sj.mp.4001939.

Myruski, S., Bonanno, G.A., Cho, H., Fan, B., Dennis-Tiwary, T.A., 2019. The late positive potential as a neurocognitive index of emotion regulatory flexibility. Biol. Psychol. 148, 107768. https://doi.org/10.1016/j.biopsycho.2019.107768.

Nelson, B.D., Hajcak, G., Shankman, S.A., 2015a. Event-related potentials to acoustic startle probes during the anticipation of predictable and unpredictable threat. Psychophysiology 52, 887–894. https://doi.org/10.1111/psyp.12418.

Nelson, B.D., Weinberg, A., Pawluk, J., Gawlowska, M., Proudfit, G.H., 2015b. An event-related potential investigation of fear generalization and intolerance of uncertainty. Behav. Ther. 46, 661–670. https://doi.org/10.1016/j.beth.2014.09.010.

Notterman, J.M., Schoenfeld, W.N., Bersh, P.J., 1952. Conditioned heart rate response in human beings during experimental anxiety. J. Comp. Physiol. Psychol. 45, 1–8. https://doi.org/10.1037/h0060870.

O'Brien, F., Cousineau, D., 2014. Representing error bars in within-subject designs in typical software packages. Quant. Method Psychol. 10, 56–67. https://doi.org/10.20982/tqmp.10.1.p056.

Obrist, P.A., 1976. Presidential Address, 1975. The cardiovascular-behavioral interaction – as it appears today. Psychophysiology 13, 95–107. https://doi.org/10.1111/j.1469-8986.1976.tb00081.x.

Olofsson, J.K., Nordin, S., Sequeira, H., Polich, J., 2008. Affective picture processing: an integrative review of ERP findings. Biol. Psychol. 77, 247–265. https://doi.org/10.1016/j.biopsycho.2007.11.006.

Pace-Schott, E.F., Germain, A., Milad, M.R., 2015. Effects of sleep on memory for conditioned fear and fear extinction. Psychol. Bull. 141, 835–857. https://doi.org/10.1037/bul0000014.

Palermo, R., Rhodes, G., 2007. Are you always on my mind? A review of how face perception and attention interact. Neuropsychologia 45, 75–92. https://doi.org/10.1016/j.neuropsychologia.2006.04.025.

Panitz, C., Hermann, C., Mueller, E.M., 2015. Conditioned and extinguished fear modulate functional corticocardiac coupling in humans. Psychophysiology 52, 1351–1360. https://doi.org/10.1111/psyp.12498.

Panitz, C., Sperl, M.F.J., Hennig, J., Klucken, T., Hermann, C., Mueller, E.M., 2018. Fearfulness, neuroticism/anxiety, and COMT Val158Met in long-term fear conditioning and extinction. Neurobiol. Learn. Mem. 155, 7–20. https://doi.org/10.1016/j.nlm.2018.06.001.

Parsons, R.G., Ressler, K.J., 2013. Implications of memory modulation for post-traumatic stress and fear disorders. Nat. Neurosci. 16, 146–153. https://doi.org/10.1038/nn.3296.

Pastor, M.C., Bradley, M.M., Löw, A., Versace, F., Moltó, J., Lang, P.J., 2008. Affective picture perception: emotion, context, and the late positive potential. Brain Res. 1189, 145–151. https://doi.org/10.1016/j.brainres.2007.10.072.

Pastor, M.C., Rehbein, M.A., Junghöfer, M., Poy, R., López, R., Moltó, J., 2015. Facing challenges in differential classical conditioning research: benefits of a hybrid design for simultaneous electrodermal and electroencephalographic recording. Front. Hum. Neurosci. 9, 336. https://doi.org/10.3389/fnhum.2015.00336.

Pavlov, Y.G., Kotchoubey, B., 2019. Classical conditioning in oddball paradigm: a comparison between aversive and name conditioning. Psychophysiology 56, 13370. https://doi.org/10.1111/psyp.13370.

Pearce, J.M., Hall, G., 1980. A model for Pavlovian learning: variations in the effectiveness of conditioned but not of unconditioned stimuli. Psychol. Rev. 87, 532–552. https://doi.org/10.1037/0033-295x.87.6.532.

Perrin, F., Pernier, J., Bertrand, O., Echallier, J.F., 1989. Spherical splines for scalp potential and current density mapping. Electroencephalogr. Clin. Neurophysiol. 72, 184–187. https://doi.org/10.1016/0013-4694(89)90180-6.

Pizzagalli, D.A., Greischar, L.L., Davidson, R.J., 2003. Spatio-temporal dynamics of brain mechanisms in aversive classical conditioning: high-density event-related potential and brain electrical tomography analyses. Neuropsychologia 41, 184–194. https://doi.org/10.1016/S0028-3932(02)00148-3.

Pourtois, G., Grandjean, D., Sander, D., Vuilleumier, P., 2004. Electrophysiological correlates of rapid spatial orienting towards fearful faces. Cereb. Cortex 14, 619–633. https://doi.org/10.1093/cercor/bhh023.

Pourtois, G., Schettino, A., Vuilleumier, P., 2013. Brain mechanisms for emotional influences on perception and attention: what is magic and what is not. Biol. Psychol. 92, 492–512. https://doi.org/10.1016/j.biopsycho.2012.02.007.

Ramanathan, K.R., Jin, J., Giustino, T.F., Payne, M.R., Maren, S., 2018. Prefrontal projections to the thalamic nucleus reuniens mediate fear extinction. Nat. Commun. 9, 4527. https://doi.org/10.1038/s41467-018-06970-z.

Rauss, K., Schwartz, S., Pourtois, G., 2011. Top-down effects on early visual processing in humans: a predictive coding framework. Neurosci. Biobehav. Rev. 35, 1237–1253. https://doi.org/10.1016/j.neubiorev.2010.12.011.

Rescorla, R.A., Wagner, A.R., 1972. A theory of Pavlovian conditioning: variations in the effectiveness of reinforcement and nonreinforcement. In: Black, A.H., Prokasy, W.F. (Eds.), Classical Conditioning II: Current Theory and Research. Appleton-Century Press, New York, NY, pp. 64–99.

Rigoulot, S., Delplanque, S., Despretz, P., Defoort-Dhellemmes, S., Honoré, J., Sequeira, H., 2008. Peripherally presented emotional scenes: a spatiotemporal analysis of early ERP responses. Brain Topogr. 20, 216–223. https://doi.org/10.1007/s10548-008-0050-9.

Roelofs, K., 2017. Freeze for action: neurobiological mechanisms in animal and human freezing. Philos. Trans. R. Soc. Lond. B Biol. Sci. 372, 20160206. https://doi.org/10.1098/rstb.2016.0206.

Roesmann, K., Wiens, N., Winker, C., Rehbein, M.A., Wessing, I., Junghoefer, M., 2020. Fear generalization of implicit conditioned facial features – behavioral and magnetoencephalographic correlates. NeuroImage 205, 116302. https://doi.org/10.1016/j.neuroimage.2019.116302.

Rossion, B., Jacques, C., 2012. The N170: understanding the time course of face perception in the human brain. In: Luck, S.J., Kappenman, E.S. (Eds.), The Oxford Handbook of Event-Related Potential Components. Oxford University Press, New York, NY, pp. 115–141. https://doi.org/10.1093/oxfordhb/9780195374148.013.0064.

Rotshtein, P., Richardson, M.P., Winston, J.S., Kiebel, S.J., Vuilleumier, P., Eimer, M., Driver, J., Dolan, R.J., 2010. Amygdala damage affects event-related potentials for fearful faces at specific time windows. Hum. Brain Mapp. 31, 1089–1105. https://doi.org/10.1002/hbm.20921.

Sabatinelli, D., Lang, P.J., Bradley, M.M., Costa, V.D., Keil, A., 2009. The timing of emotional discrimination in human amygdala and ventral visual cortex. J. Neurosci. 29, 14864–14868. https://doi.org/10.1523/JNEUROSCI.3278-09.2009.

Schindler, S., Bruchmann, M., Bublatzky, F., Straube, T., 2019. Modulation of face- and emotion-selective ERPs by the three most common types of face image manipulations. Soc. Cogn. Affect. Neurosci. 14, 493–503. https://doi.org/10.1093/scan/nsz027.

Schindler, S., Bruchmann, M., Steinweg, A.-L., Moeck, R., Straube, T., 2020. Attentional conditions differentially affect early, intermediate and late neural responses to fearful and neutral faces. Soc. Cogn. Affect. Neurosci. https://doi.org/10.1093/scan/nsaa098.

Schindler, S., Bublatzky, F., 2020. Attention and emotion: an integrative review of emotional face processing as a function of attention. Cortex 130, 362–386. https://doi.org/10.1016/j.cortex.2020.06.010.

Schroder, H.S., Nickels, S., Cardenas, E., Breiger, M., Perlo, S., Pizzagalli, D.A., 2019. Optimizing assessments of post-error slowing: a neurobehavioral investigation of a flanker task. Psychophysiology 13473. https://doi.org/10.1111/psyp.13473.

Schupp, H., Cuthbert, B., Bradley, M., Hillman, C., Hamm, A., Lang, P., 2004. Brain processes in emotional perception: motivated attention. Cogn. Emot. 18, 593–611. https://doi.org/10.1080/02699930341000239.

Schupp, H.T., Flaisch, T., Stockburger, J., Junghöfer, M., 2006. Emotion and attention: event-related brain potential studies. Prog. Brain Res. 156, 31–51. https://doi.org/10.1016/S0079-6123(06)56002-9.

Schweinberger, S.R., 2011. Neurophysiological correlates of face recognition. In: Calder, A.J., Rhodes, G., Johnson, M.H., Haxby, J.V. (Eds.), The Oxford Handbook of Face Perception. Oxford University Press, New York, NY, pp. 345–366 https://doi.org/10.1093/oxfordhb/9780199559053.013.0018.

Sehlmeyer, C., Schöning, S., Zwitserlood, P., Pfleiderer, B., Kircher, T., Arolt, V., Konrad, C., 2009. Human fear conditioning and extinction in neuroimaging: a systematic review. PLoS One 4, 5865. https://doi.org/10.1371/journal.pone.0005865.

Seligowski, A.V., Bondy, E., Singleton, P., Orcutt, H.K., Ressler, K.J., Auerbach, R.P., 2018. Testing neurophysiological markers related to fear-potentiated startle. Psychiatry Res. 267, 195–200. https://doi.org/10.1016/j.psychres.2018.06.023.

Shackman, A.J., Maxwell, J.S., McMenamin, B.W., Greischar, L.L., Davidson, R.J., 2011. Stress potentiates early and attenuates late stages of visual processing. J. Neurosci. 31, 1156–1161. https://doi.org/10.1523/JNEUROSCI.3384-10.2011.

Sperl, M.F.J., Panitz, C., Hermann, C., Mueller, E.M., 2016. A pragmatic comparison of noise burst and electric shock unconditioned stimuli for fear conditioning research with many trials. Psychophysiology 53, 1352–1365. https://doi.org/10.1111/psyp.12677.

Sperl, M.F.J., Panitz, C., Rosso, I.M., Dillon, D.G., Kumar, P., Hermann, A., Whitton, A.E., Hermann, C., Pizzagalli, D.A., Mueller, E.M., 2019. Fear extinction recall modulates human frontomedial theta and amygdala activity. Cereb. Cortex 29, 701–715. https://doi.org/10.1093/cercor/bhx353.

Stange, J.P., MacNamara, A., Barnas, O., Kennedy, A.E., Hajcak, G., Phan, K.L., Klumpp, H., 2017. Neural markers of attention to aversive pictures predict response to cognitive behavioral therapy in anxiety and depression. Biol. Psychol. 123, 269–277. https://doi.org/10.1016/j.biopsycho.2016.10.009.

Stegmann, Y., Ahrens, L., Pauli, P., Keil, A., Wieser, M.J., 2020. Social aversive generalization learning sharpens the tuning of visuocortical neurons to facial identity cues. eLife 9, 55204. https://doi.org/10.7554/eLife.55204.

Steinberg, C., Bröckelmann, A.-K., Rehbein, M., Dobel, C., Junghöfer, M., 2013. Rapid and highly resolving associative affective learning: convergent electro- and magnetoencephalographic evidence from vision and audition. Biol. Psychol. 92, 526–540. https://doi.org/10.1016/j.biopsycho.2012.02.009.

Steinberg, C., Dobel, C., Schupp, H.T., Kissler, J., Elling, L., Pantev, C., Junghöfer, M., 2012. Rapid and highly resolving: affective evaluation of olfactorily conditioned faces. J. Cogn. Neurosci. 24, 17–27. https://doi.org/10.1162/jocn_a_00067.

Stolarova, M., Keil, A., Moratti, S., 2006. Modulation of the C1 visual event-related component by conditioned stimuli: evidence for sensory plasticity in early affective perception. Cereb. Cortex 16, 876–887. https://doi.org/10.1093/cercor/bhj031.

Stolz, C., Endres, D., Mueller, E.M., 2019. Threat-conditioned contexts modulate the late positive potential to faces – a mobile EEG/virtual reality study. Psychophysiology 56, 13308. https://doi.org/10.1111/psyp.13308.

Tamietto, M., Gelder, B.de, 2010. Neural bases of the non-conscious perception of emotional signals. Nat. Rev. Neurosci. 11, 697–709. https://doi.org/10.1038/nrn2889.

Thigpen, N.N., Bartsch, F., Keil, A., 2017. The malleability of emotional perception: short-term plasticity in retinotopic neurons accompanies the formation of perceptual biases to threat. J. Exp. Psychol. Gen. 146, 464–471. https://doi.org/10.1037/xge0000283.

Tottenham, N., Tanaka, J.W., Leon, A.C., McCarry, T., Nurse, M., Hare, T.A., Marcus, D.J., Westerlund, A., Casey, B.J., Nelson, C., 2009. The NimStim set of facial expressions: judgments from untrained research participants. Psychiatry Res. 168, 242–249. https://doi.org/10.1016/j.psychres.2008.05.006.

Tovote, P., Fadok, J.P., Lüthi, A., 2015. Neuronal circuits for fear and anxiety. Nat. Rev. Neurosci. 16, 317–331. https://doi.org/10.1038/nrn3945.

Tzovara, A., Korn, C.W., Bach, D.R., 2018. Human Pavlovian fear conditioning conforms to probabilistic learning. PLoS Comput. Biol. 14, e1006243. https://doi.org/10.1371/journal.pcbi.1006243.

Valentini, E., Betti, V., Hu, L., Aglioti, S.M., 2013. Hypnotic modulation of pain perception and of brain activity triggered by nociceptive laser stimuli. Cortex 49, 446–462. https://doi.org/10.1016/j.cortex.2012.02.005.

Vila, J., Guerra, P., Muñoz, M.A., Vico, C., Viedma-del Jesús, M.I., Delgado„ L.C., Perakakis, P., Kley, E., Mata, J.L., Rodríguez, S., 2007. Cardiac defense: from attention to action. Int. J. Psychophysiol. 66, 169–182. https://doi.org/10.1016/j.ijpsycho.2007.07.004.

Voulo, M.E., Parsons, R.G., 2017. Response-specific sex difference in the retention of fear extinction. Learn. Mem. 24, 245–251. https://doi.org/10.1101/lm.045641.117.

Vuilleumier, P., 2009. The role of the human amygdala in perception and attention. In: Whalen, P.J., Phelps, E.A. (Eds.), The Human Amygdala. Guilford Press, New York, NY, pp. 220–249.

Vuilleumier, P., Richardson, M.P., Armony, J.L., Driver, J., Dolan, R.J., 2004. Distant influences of amygdala lesion on visual cortical activation during emotional face processing. Nat. Neurosci. 7, 1271–1278. https://doi.org/10.1038/nn1341.

Wang, C., Ma, Y., Han, S., 2014. Self-construal priming modulates pain perception: event-related potential evidence. Cogn. Neurosci. 5, 3–9. https://doi.org/10.1080/17588928.2013.797388.

Wang, C., Tian, J., 2018. Reminders of mortality alter pain-evoked potentials in a Chinese sample. Front. Psychol. 9, 1667. https://doi.org/10.3389/fpsyg.2018.01667.

Watters, A.J., Rupert, P.E., Wolf, D.H., Calkins, M.E., Gur, R.C., Gur, R.E., Turetsky, B.I., 2018. Social aversive conditioning in youth at clinical high risk for psychosis and with psychosis: an ERP study. Schizophr. Res. 202, 291–296. https://doi.org/10.1016/j.schres.2018.06.027.

Weinberg, A., Hajcak, G., 2011. Electrocortical evidence for vigilance-avoidance in generalized anxiety disorder. Psychophysiology 48, 842–851. https://doi.org/10.1111/j.1469-8986.2010.01149.x.

Weinberg, A., Perlman, G., Kotov, R., Hajcak, G., 2016. Depression and reduced neural response to emotional images: distinction from anxiety, and importance of symptom dimensions and age of onset. J. Abnorm. Psychol. 125, 26–39. https://doi.org/10.1037/abn0000118.

Weinberg, A., Venables, N.C., Proudfit, G.H., Patrick, C.J., 2015. Heritability of the neural response to emotional pictures: evidence from ERPs in an adult twin sample. Soc. Cogn. Affect. Neurosci. 10, 424–434. https://doi.org/10.1093/scan/nsu059.

Whitton, A.E., Kakani, P., Foti, D., Van't Veer, A., Haile, A., Crowley, D.J., Pizzagalli, D.A., 2016. Blunted neural responses to reward in remitted major depression: a high-density event-related potential study. Biol. Psychiatry Cogn. Neurosci. Neuroimaging 1, 87–95. https://doi.org/10.1016/j.bpsc.2015.09.007.

Wieser, M.J., Keil, A., 2020. Attentional threat biases and their role in anxiety: a neurophysiological perspective. Int. J. Psychophysiol. 153, 148–158. https://doi.org/10.1016/j.ijpsycho.2020.05.004.

Wills, A.J., 2009. Prediction errors and attention in the presence and absence of feedback. Curr. Dir. Psychol. Sci. 18, 95–100. https://doi.org/10.1111/j.1467-8721.2009.01616.x.

Wills, A.J., Lavric, A., Croft, G.S., Hodgson, T.L., 2007. Predictive learning, prediction errors, and attention: evidence from event-related potentials and eye tracking. J. Cogn. Neurosci. 19, 843–854. https://doi.org/10.1162/jocn.2007.19.5.843.

Winkler, I., Debener, S., Müller, K.-R., Tangermann, M., 2015. On the influence of high-pass filtering on ICA-based artifact reduction in EEG-ERP. Annu. Int. Conf. I.E.E.E. Eng. Med. Biol. Soc. 37, 4101–4105. https://doi.org/10.1109/EMBC.2015.7319296.

Yamaguchi, S., Knight, R.T., 1991. P300 generation by novel somatosensory stimuli. Electroencephalogr. Clin. Neurophysiol. 78, 50–55. https://doi.org/10.1016/0013-4694(91)90018-Y.

Yin, S., Liu, Y., Petro, N.M., Keil, A., Ding, M., 2018. Amygdala adaptation and temporal dynamics of the salience network in conditioned fear: a single-trial fMRI study. eNeuro 5, ENEURO.0445–17.2018. https://doi.org/10.1523/ENEURO.0445-17.2018.

Zaslansky, R., Sprecher, E., Tenke, E.C., Hemli, A.J., Yarnitsky, D., 1996. The P300 in pain evoked potentials. Pain 66, 39–49. https://doi.org/10.1016/0304-3959(96)03020-5.